NMSSM Tevatron/LHC Scenarios: Motivation and Phenomenology

Jack Gunion
Davis Institute for High Energy Physics, U.C. Davis

TeV4LHC, Fermilab, December 14, 2004

News from the NMSSM and Beyond

- **NMSSM Naturalness Issues**
- **NMSSM Baryogenesis**
- **NMHDECAY**
- **NMSSM LHC and Tevatron Phenomenology**

MSSM problems:

- **The MSSM is being pushed into parameter regions characterized by substantial fine tuning and a "little" hierarchy problem (i.e. large stop masses) in order to have a heavy enough Higgs boson for consistency with LEP limits.**
- **A strong phase transition for baryogenesis is hard to arrange when the Higgs is heavy and the stops are heavy.**
- **No really attractive explanation for the μ parameter has emerged.**

One can marginally escape all but the last of these problems if significant Higgs sector CP violation is introduced through SUSY loops. However, I will propose that it is time to adopt the NMSSM as the baseline supersymmetric model.

The NMSSM phenomenology is considerably richer than that of the MSSM in many important ways. The focus here is on Higgs physics.

References

[1] H. P. Nilles, M. Srednicki and D. Wyler, Phys. Lett. B 120 (1983) 346.
J. M. Frere, D. R. T. Jones and S. Raby, Nucl. Phys. B 222 (1983) 11.
J. P. Derendinger and C. A. Savoy, Nucl. Phys. B 237 (1984) 307.
J. R. Ellis, J. F. Gunion, H. E. Haber, L. Roszkowski and F. Zwirner, Phys. Rev. D 39 (1989) 844.
M. Drees, Int. J. Mod. Phys. A 4 (1989) 3635.
U. Ellwanger, M. Rausch de Traubenberg and C. A. Savoy, Phys. Lett. B 315 (1993) 331 [arXiv:hep-ph/9307322], and Nucl. Phys. B 492 (1997) 21 [arXiv:hep-ph/9611251],
S. F. King and P. L. White, Phys. Rev. D 52 (1995) 4183 [arXiv:hep-ph/9505326].
F. Franke and H. Fraas, Int. J. Mod. Phys. A 12 (1997) 479 [arXiv:hep-ph/9512366].

[2] M. Bastero-Gil, C. Hugonie, S. F. King, D. P. Roy and S. Vempati, Phys. Lett. B 489 (2000) 359 [arXiv:hep-ph/0006198].

[3] S. F. King and P. L. White, Phys. Rev. D 52, 4183 (1995) [arXiv:hep-ph/9505326].

[4] S. A. Abel, S. Sarkar and P. L. White, Nucl. Phys. B 454 (1995) 663 [arXiv:hep-ph/9506359].

[5] S. A. Abel, Nucl. Phys. B 480 (1996) 55 [arXiv:hep-ph/9609323],
C. Panagiotakopoulos and K. Tamvakis, Phys. Lett. B 446 (1999) 224 [arXiv:hep-ph/9809475].

[6] H. P. Nilles, M. Srednicki and D. Wyler, Phys. Lett. B 124 (1983) 337,
U. Ellwanger, Phys. Lett. B 133 (1983) 187,
J. Bagger and E. Poppitz, Phys. Rev. Lett. 71 (1993) 2380 [arXiv:hep-ph/9307317],
J. Bagger, E. Poppitz and L. Randall, Nucl. Phys. B 455 (1995) 59 [arXiv:hep-ph/9505244].

[7] U. Ellwanger, Phys. Lett. B 303 (1993) 271 [arXiv:hep-ph/9302224].

[8] P. N. Pandita, Phys. Lett. B 318 (1993) 338,
T. Elliott, S. F. King and P. L. White, Phys. Rev. D 49 (1994) 2435 [arXiv:hep-ph/9308309],

[9] J. i. Kamoshita, Y. Okada and M. Tanaka, Phys. Lett. B 328 (1994) 67 [arXiv:hep-ph/9402278],
U. Ellwanger, M. Rausch de Traubenberg and C. A. Savoy, Z. Phys. C 67 (1995) 665 [arXiv:hep-ph/9502206],
S. F. King and P. L. White, Phys. Rev. D 53 (1996) 4049 [arXiv:hep-ph/9508346],
S. W. Ham, S. K. Oh and B. R. Kim, J. Phys. G 22 (1996) 1575 [arXiv:hep-ph/9604243],
D. J. Miller, R. Nevzorov and P. M. Zerwas, Nucl. Phys. B 681 (2004) 3 [arXiv:hep-ph/0304049],

G. Hiller, arXiv:hep-ph/0404220.

[10] U. Ellwanger, J. F. Gunion, C. Hugonie and S. Moretti, "NMSSM Higgs discovery at the LHC," arXiv:hep-ph/0401228, and "Towards a no-lose theorem for NMSSM Higgs discovery at the LHC," arXiv:hep-ph/0305109.

[11] D. J. Miller and S. Moretti, "An interesting NMSSM scenario at the LHC and LC," arXiv:hep-ph/0403137.

[12] G. K. Yeghian, "Upper bound on the lightest Higgs mass in supersymmetric theories," arXiv:hep-ph/9904488.

[13] U. Ellwanger and C. Hugonie, Eur. Phys. J. C 25 (2002) 297 [arXiv:hep-ph/9909260].

[14] U. Ellwanger, J. F. Gunion and C. Hugonie, arXiv:hep-ph/0406215.

[15] J. R. Ellis, J. F. Gunion, H. E. Haber, L. Roszkowski and F. Zwirner, Phys. Rev. D 39, 844 (1989).

[16] G.L. Kane and S.F. King, Phys. Lett. B451 (1999) 113.
See also: S. Dimopoulos and G.F. Giudice, Phys. Lett. B357 (1995) 573; P.H. Chankowski, J. Ellis, S. Pokorski, Phys. Lett. B423 (1998) 327; P.H. Chankowski, J. Ellis, M. Olechowski, S. Pokorski, Nucl. Phys. B544 (1999) 39.

[17] A. Menon, D. E. Morrissey and C. E. M. Wagner, Phys. Rev. D 70, 035005 (2004) [arXiv:hep-ph/0404184].

[18] S. J. Huber and M. G. Schmidt, Nucl. Phys. B 606, 183 (2001) [arXiv:hep-ph/0003122].

[19] J. F. Gunion, H. E. Haber and T. Moroi, arXiv:hep-ph/9610337.

[20] J. Dai, J. F. Gunion and R. Vega, Phys. Rev. Lett. 71, 2699 (1993) [arXiv:hep-ph/9306271].

[21] J. Dai, J. F. Gunion and R. Vega, Phys. Lett. B 345, 29 (1995) [arXiv:hep-ph/9403362].

[22] D. L. Rainwater and D. Zeppenfeld, Phys. Rev. D 60, 113004 (1999) [Erratum-ibid. D 61, 099901 (2000)] [arXiv:hep-ph/9906218].

[23] T. Plehn, D. L. Rainwater and D. Zeppenfeld, Phys. Lett. B 454, 297 (1999) [arXiv:hep-ph/9902434].

[24] D. L. Rainwater, D. Zeppenfeld and K. Hagiwara, Phys. Rev. D 59, 014037 (1999) [arXiv:hep-ph/9808468].

[25] B. A. Dobrescu, G. Landsberg and K. T. Matchev, Phys. Rev. D 63, 075003 (2001) [arXiv:hep-ph/0005308].

[26] U. Ellwanger, J. F. Gunion and C. Hugonie, arXiv:hep-ph/0111179.

[27] U. Ellwanger, J. F. Gunion, C. Hugonie and S. Moretti, arXiv:hep-ph/0305109.

[28] J. F. Gunion and M. Szleper, arXiv:hep-ph/0409208.

The NMSSM

- The Next to Minimal Supersymmetric Standard Model (NMSSM [1, 2, 3, 4, 5, 7, 8, 9, 10, 11, 12, 13]) provides a very elegant solution to the μ problem of the MSSM via the introduction of a singlet superfield $\widehat{S}$.

  For the simplest possible scale invariant form of the superpotential, the scalar component of $\widehat{S}$ acquires naturally a vacuum expectation value of the order of the SUSY breaking scale, giving rise to a value of μ of order the electroweak scale.

  The NMSSM is actually the simplest supersymmetric extension of the standard model in which the electroweak scale originates from the SUSY breaking scale only.

- In addition, the NMSSM renders the "little fine tuning problem" of the MSSM, originating from the non-observation of a neutral CP-even Higgs boson at LEP II, less severe [2]. Fine-tuning was also studied earlier in [3]. Our discussion here comes to rather different conclusions as compared to either reference.

- A possible cosmological domain wall problem [4] can be avoided by introducing suitable non-renormalizable operators [5] that do not generate dangerously large singlet tadpole diagrams [6].

Hence, the phenomenology of the NMSSM deserves to be studied at least as fully and precisely as that of the MSSM.

Its particle content differs from the MSSM by the addition of one CP-even and one CP-odd state in the neutral Higgs sector (assuming CP conservation), and one additional neutralino. Thus, the physics of the Higgs bosons – masses, couplings and branching ratios [1, 7, 8, 9, 10, 11, 12, 13] can differ significantly from the MSSM.

I will be following the conventions of Ellwanger, Hugonie, JFG [14]. The NMSSM parameters are as follows.

a) Apart from the usual quark and lepton Yukawa couplings, the scale invariant superpotential is

$$\lambda\ \widehat{S}\widehat{H_u}\widehat{H_d} + \frac{\kappa}{3}\ \widehat{S}^3 \tag{1}$$

depending on two dimensionless couplings λ, κ beyond the MSSM. (Hatted capital letters denote superfields, and unhatted capital letters will denote their scalar components).

b) The associated trilinear soft terms are

$$\lambda A_\lambda S H_u H_d + \frac{\kappa}{3} A_\kappa S^3 \,. \tag{2}$$

c) The final two input parameters are

$$\tan\beta = \langle H_u \rangle / \langle H_d \rangle \;,\; \mu_{\rm eff} = \lambda \langle S \rangle \;. \tag{3}$$

These, along with M_Z, can be viewed as determining the three SUSY breaking masses squared for H_u, H_d and S through the three minimization equations of the scalar potential.

Thus, as compared to two independent parameters in the Higgs sector of the MSSM (often chosen as $\tan\beta$ and M_A), the Higgs sector of the NMSSM is described by the six parameters

$$\lambda \;,\; \kappa \;,\; A_\lambda \;,\; A_\kappa ,\; \tan\beta \;,\; \mu_{\rm eff} \;. \tag{4}$$

We will choose sign conventions for the fields such that λ and $\tan\beta$ are positive, while κ, A_λ, A_κ and $\mu_{\rm eff}$ should be allowed to have either sign.

In addition, values for the gaugino masses and of the soft terms related to the squarks and sleptons that contribute to the radiative corrections in the Higgs sector and to the Higgs decay widths must be input.

Fine Tuning

w. Radovan Dermisek

The MSSM

Sample discussions of the issues appear in the papers cited in [16].

A typical and useful discussion for the MSSM is that given by Kane and King. They find that even at high $\tan\beta$ it is difficult to reduce fine tuning

$$F = \mathrm{Max}_a F_a \equiv \mathrm{Max}_a \left| \frac{d \log m_Z^2}{d \log a} \right| , \quad (5)$$

where the parameters a are the GUT scale soft-SUSY-breaking parameters and the μ parameter, below the level of about 50 for $M_3 = 200$ GeV. A typical graph was that presented for $m_0 = 100$ GeV and $M_2 = M_1 = 200$, and $M_3 = 200$, 150 and 100 GeV. (All parameters given are GUT scale

values.)

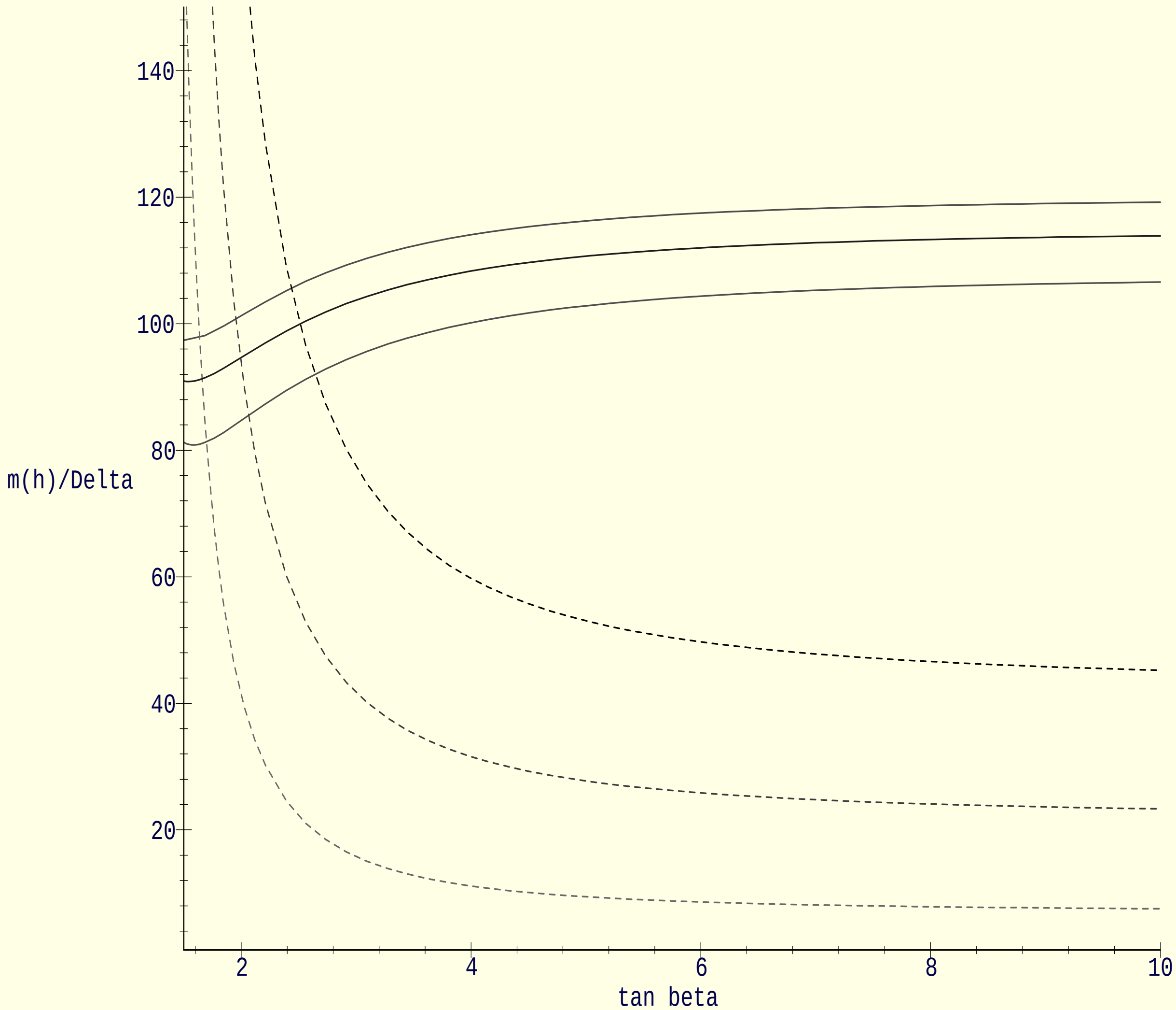

Figure 1: Higgs mass m_h and F_μ as functions of $\tan\beta$ for $m_0 = 100$ GeV, $M_{1,2} = 200$ GeV and $M_3 = 200$, 150 and 100 GeV.

One can write down formulae for m_Z^2 and F_μ. The procedure is to evolve GUT-scale parameters down to m_Z and then insert the evolution results into

$$\frac{1}{2}m_Z^2 = -\mu^2 + \frac{m_{H_d}^2 - t_\beta^2 m_{H_u}^2}{t_\beta^2 - 1}\,. \tag{6}$$

For example, at $\tan\beta = 2.5$ they find (GUT parameters again):

$$\begin{aligned}\frac{1}{2}m_Z^2 \quad = \quad & -0.87\mu^2 + 3.6M_3^2 - 0.12M_2^2 + 0.007M_1^2 - 0.71m_{H_u}^2 + 0.10m_{H_d}^2 \\ & +0.48(m_Q^2 + m_U^2) - 0.34A_tM_3 + 0.25M_2M_3 + small\,. \end{aligned} \tag{7}$$

From this you already see the problem with large M_3^2. You must have carefully tuned cancellation to get m_Z^2 right. Of course, one cannot rule out the possibility that such cancellation is natural in particular models that have a built in correlation between μ and M_3, for example.

The NMSSM

We now contrast this to the NMSSM situation. Here, the computation of m_Z^2 is much more complicated. Some results on this have appeared in refs. [2] and [3], but I will claim they missed the most interesting part of parameter space with the smallest finetuning. We start with

$$V = \lambda^2(h_u^2 s^2 + h_d^2 s^2 + h_u^2 h_d^2) + \kappa^2 s^4 - 2\lambda\kappa h_u h_d s^2 - 2\lambda A_\lambda\, h_u h_d s$$
$$+\frac{2}{3}\kappa A_\kappa s^3 + m_{H_u}^2 h_u^2 + m_{H_d}^2 h_d^2 + m_S^2 s^2 + \frac{1}{4} g^2 (h_u^2 - h_d^2)^2 \,. \quad (8)$$

In the above, h_u and h_d are the vevs of the up and down type Higgs fields (without any $\sqrt{2}$) and s is the vev of the singlet Higgs field in the normalizations of NMHDECAY. (What I call g^2 is $g^2 \equiv \frac{1}{2}(g_2^2 + g'^2)$ so that $m_Z^2 = g^2(h_u^2 + h_d^2)$.)

One must then solve the minimization equations

$$\frac{\partial V}{\partial h_u} = 0, \quad \frac{\partial V}{\partial h_d} = 0, \quad \frac{\partial V}{\partial s} = 0 \quad (9)$$

for the soft masses squared and explore combinations thereof for reexpressing the minimization conditions. One finds

$$m_{H_u}^2 = \frac{1}{2h_u}\left(g^2h_d^2h_u - g^2h_u^3 - 2h_d^2h_u\lambda^2 + 2A_\lambda h_d\lambda s + 2h_d\kappa\lambda s^2 - 2h_u\lambda^2 s^2\right) \quad (10)$$

$$m_{H_d}^2 = \frac{1}{2h_d}\left(g^2h_dh_u^2 - g^2h_d^3 - 2h_dh_u^2\lambda^2 + 2A_\lambda h_u\lambda s + 2h_u\kappa\lambda s^2 - 2h_d\lambda^2 s^2\right) \quad (11)$$

$$m_S^2 = \frac{1}{s}\left(\lambda A_\lambda h_dh_u + 2h_dh_u\kappa\lambda s - h_d^2\lambda^2 s - h_u^2\lambda^2 s - \kappa A_\kappa s^2 - 2\kappa^2 s^3\right) \quad (12)$$

One then defines

$$\mu_{\rm eff} = \lambda s\,, \qquad \tan\beta \equiv \frac{h_u}{h_d}\,. \quad (13)$$

It is then easy to eliminate terms linear in s to find that

$$\frac{1}{2}m_Z^2 = -\mu_{\rm eff}^2 + \frac{m_{H_d}^2 - \tan^2\beta m_{H_u}^2}{\tan^2\beta - 1}\,. \quad (14)$$

However, $\mu_{\rm eff}$ is not a fundamental parameter in this case. Taking $(\kappa\lambda/\tan\beta-$

$\lambda^2)$(11) $-(\kappa\lambda\tan\beta-\lambda^2)$ (10), we obtain a second equation

$$\begin{aligned} &\kappa\lambda\left(\frac{1}{\tan\beta}m_{H_d}^2-m_{H_u}^2\tan\beta\right)-\lambda^2\left(m_{H_d}^2-m_{H_u}^2\right) \\ &=\frac{1}{2}m_Z^2\frac{\tan^2\beta-1}{\tan^2\beta+1}\left[\kappa\lambda\left(\frac{1}{\tan\beta}+\tan\beta\right)-2\lambda^2+\frac{2}{g^2}\lambda^4\right] \\ &+\mu_{eff}A_\lambda\lambda^2\left(\frac{1}{\tan\beta}-\tan\beta\right) \end{aligned} \tag{15}$$

Let's make it simpler by defining

$$a = -\frac{1}{2}\frac{\tan^2\beta-1}{\tan^2\beta+1}\left[\kappa\lambda\left(\frac{1}{\tan\beta}+\tan\beta\right)-2\lambda^2+\frac{2}{g^2}\lambda^4\right] \tag{16}$$

$$b = \frac{1}{\tan\beta}k\lambda\left(m_{Hd}^2-m_{Hu}^2\tan^2\beta\right)-\lambda^2\left(m_{Hd}^2-m_{Hu}^2\right) \tag{17}$$

$$c = A_\lambda\lambda^2\left(\frac{1}{\tan\beta}-\tan\beta\right) \tag{18}$$

so that it is simply

$$aM_Z^2+b=c\mu_{eff}. \tag{19}$$

Squaring this equation and plugging in μ_{eff} from Eq. (14) we can eliminate μ_{eff} completely, and we obtain a quadratic equation for M_Z^2 with coefficients given in terms of soft susy breaking parameters:

$$AM_Z^4 + BM_Z^2 + C = 0, \tag{20}$$

where

$$A = a^2 \tag{21}$$

$$B = 2ab + c^2/2 \tag{22}$$

$$C = b^2 + c^2\frac{m_{Hd}^2 - m_{Hu}^2 \tan^2\beta}{1 - \tan^2\beta}. \tag{23}$$

This is the equivalent formula to that in the case of the MSSM. A, B, and C can be expressed in terms of SSB parameters at the GUT scale; the only difference is that it is a quadratic equation. Therefore there are two solutions:

$$m_Z^2 = \frac{1}{2A}\left(-B \pm \sqrt{B^2 - 4AC}\right). \tag{24}$$

Only one applies for any given set of parameter choices.

To explore fine tuning, we begin at scale m_Z.

- We fix λ and κ, choose values for $\tan\beta$ and $\tan\gamma \equiv s/v$, and of course fix $h_u^2 + h_d^2 = v^2$. In the NMHDECAY conventions employed, $\lambda > 0$ and $\tan\beta > 0$, but κ can have either sign.

  We also find it easiest to fix the soft-SUSY-breaking parameters A_λ, A_κ, and $A_t = A_b$ at scale m_Z.

- We also wish consider given GUT scale values for

$$M_1, \quad M_2, \quad M_3, \quad m_Q^2, \quad m_U^2, \quad m_D^2, \quad m_L^2, \quad \text{and} \quad m_E^2 . \tag{25}$$

  These we will take to have respective universal values.

- We use the usual back and forth RGE iteration approach to determine the values of m_Q^2, m_U^2, m_D^2, m_L^2, and m_E^2 at scale m_Z that are consistent with these GUT scale values and the scale-m_Z values for $\lambda, \kappa, \tan\beta, \tan\gamma, A_t, A_\lambda, A_\kappa$. These are then input into the Higgs multi-loop mass and analysis program.

  At the same time, we obtain $m_{H_u}^2$, $m_{H_d}^2$ and m_S^2 GUT scale values that are consistent with the choices determined by our m_Z scale inputs (which immediately fix the above quantities at scale m_Z via minimization conditions).

- We can compute the F_a by perturbing the GUT scale input a a bit, recomputing the resulting $m^2_{H_u}(m_Z)$, $m^2_{H_d}(m_Z)$, $m^2_S(m_Z)$, $A_\lambda(m_Z)$ and $A_\kappa(m_Z)$ and then reminimizing the potential, which will yield new values of m_Z (and $\tan\beta$ and $\tan\gamma$).

  We use the shifted m_Z computed as above to compute F_a.

Resulting observations

- One finds, depending upon input GUT scale parameters, that the largest of the F_a (F) can be quite modest in size even if the GUT scale parameters are quite large.

  In fact, we can always find parameter choices such that $F \sim 9 \div 10$ can be achieved, far below the MSSM values.

  (Of course, there are other choices that give large F.)

An example of small F

- **We consider Kane-King like choices:** $\tan\beta = 3$, $M_1 = M_2 = M_3 = 300~\mathrm{GeV}$ **(higher than their** $200~\mathrm{GeV}$**) and and a universal value for** $m_0^2 = m_Q^2 = m_U^2 = m_D^2 = m_L^2 = m_E^2 = (400~\mathrm{GeV})^2$**.**

- **We scan over various possible** $A_t(m_Z)$, $A_\lambda(m_Z)$ **and** $A_\kappa(m_Z)$ **values.**

- **We require** $\mu_{\mathrm{eff}} > 100~\mathrm{GeV}$ **and** $M_2(m_Z) > 100~\mathrm{GeV}$ **(to avoid a light chargino).**

A typical small F case

```
F=9.3

H masses={361, 283, 72}  P masses= {355, 17}  H+ mass= 351

At low scale
l= 0.363 k= 0.214 tanb=3. s=665    M1= -126 M2=-248 M3=-888
mHu2u=-49708.3  mHd2u=52699.7  mS2u=043036.8
mQ2=448390. mu2=106338. md2=758901. mL2=241725. me2=102443.
Au=218.3 Al=11.53 Ak=0.462

At GUT scale
l=  0.4796  k= -0.2915    Ak=  -180.5   Al=  -1008.8   Au=  -2495.4
mHu2=  1065740  mHd2=  4936.6  mS2=  19770.1
```

Our scanning statistics are still low, but it can certainly be said that a very efficient means for selecting scenarios with small F is to focus on small A_κ, which generically leads to $h_1 \to a_1 a_1$ decays as being possible and not infrequently dominant, with the h_1 being quite SM-like. Such scenarios can evade current LEP constraints (as we shall come to).

Typical expressions for the things that enter into the calculation of a, b, and c and thence A, B and C are:

```
AlMZ= 0.760 AlG - 0.353 AuG  - 0.314 M2G + 0.699 M3G + small


AkMZ=0.867 AkG - 0.375 AlG + small


mHu2MZ=  0.151 M2G^2 + 0.281 AuG M3G - 0.189 M2G M3G - 3.1 M3G^2  + 0.523 mHu2G
       - 0.43 mQ2G - 0.33 mu2G


mHd2MZ= 0.446 M2G^2 + 0.899 mHd2G + small


mS2MZ= 0.742 mS2G + small
```

Clearly, the analysis of exactly why there is cancellation in the computation of F is somewhat complex, but we are working on it. What is clear is the general fact that there is a cancellation going on for all the small fine-tuning solutions. For example, in the above case, $B = 13210$ while $\sqrt{B^2 - 4AC} = 21556$ and $m_Z^2 = (-B + \sqrt{B^2 - 4AC})/(2A)$. Thus, B

is fairly dominant (often it is very dominant) and whatever dependence on some GUT parameter is present in B, it is also present with similar strength in $\sqrt{B^2-4AC}$, implying (for the sign shown) that the change in $-B$ is compensated fairly well by the change in $\sqrt{B^2-4AC}$.

Baryogenesis in the NMSSM

w. K. Kelley

The only work on this in the literature is that of ref. [2]. Others have focused on models with different or specialized superpotentials such as $W = \lambda \widehat{S}\widehat{H}_u\widehat{H}_d + \frac{m_{12}^2}{\lambda}\widehat{S}$ [17] or $W = \lambda \widehat{S}\widehat{H}_u\widehat{H}_d + \frac{\kappa}{3}\widehat{S}^3 + \mu\widehat{H}_u\widehat{H}_d + r\widehat{S}$ [18]. We are revisiting this to see to what extent the parameter regions with $h \to aa$ decays might be preferred over other regions.

We stick to the NMSSM as already defined. We employ the usual types of machinery to evaluate the strength of the phase transition prior to introducing CP violation into the Higgs sector (either through loops or explicitly). As usual, we employ the criterion of $\frac{v}{T_c} > 1$ as being required for a strong enough phase transition (as needed for the out-of-equilibrium condition for adequate baryogenesis). We have so far only looked at top and stop loop contributions. We are in the process of putting in contributions from the neutralino and chargino sectors, etc. The results are thus quite PRELIMINARY.

As we expected, electroweak baryogenesis is more easily accommodated in the NMSSM than in the MSSM. The reasons are:

- The SM-like Higgs can be lighter and still escape detection via $h_1 \to a_1 a_1$

dominance. (Recall that a light SM-like Higgs strengthens the phase transition.)

- If you require m_{h_1} to be up near the LEP limit because $h_1 \to a_1 a_1$ decays are absent, you can succeed with a lighter $\widetilde{t}$ than in the MSSM. This is because the h_1 mass gets an extra contribution at tree level:

$$m_{h_1}^2 \leq m_Z^2 \left(\cos^2 2\beta + \frac{2\lambda^2}{g_1^2 + g_2^2} \sin^2 2\beta \right) . \tag{26}$$

which can give substantial $m_{h_1}^2$ even at tree-level for moderate $\tan\beta$. For example, for small κ and $\widetilde{X_t} = \sqrt{6}$ (maximal mixing), $m_{h_1}^2$ is maximum for $\tan\beta \sim 3$ where, depending upon κ, λ can be big enough to give $m_{h_1} \sim 130~\mathrm{GeV}$.

So far, we have kept $m_{\widetilde{t}_{1,2}} \sim 1~\mathrm{TeV}$ and explored parameter space in the region defined by:

$$\lambda \in [0.1, 0.65], \quad \kappa \in [0.1, 0.65], \quad \tan\beta \in [1.6, 3.0], \quad \mu_{\mathrm{eff}} = \lambda s \in [17.5, 350],$$
$$A_\lambda \in [-1000, 1000]~\mathrm{GeV}, \quad A_\kappa \in [-1000, 1000]~\mathrm{GeV}, \quad A_t = 1.5~\mathrm{TeV} \tag{27}$$

the latter being for roughly maximal mixing.

Below is a plot showing the $v/T_c > 1$ cases.

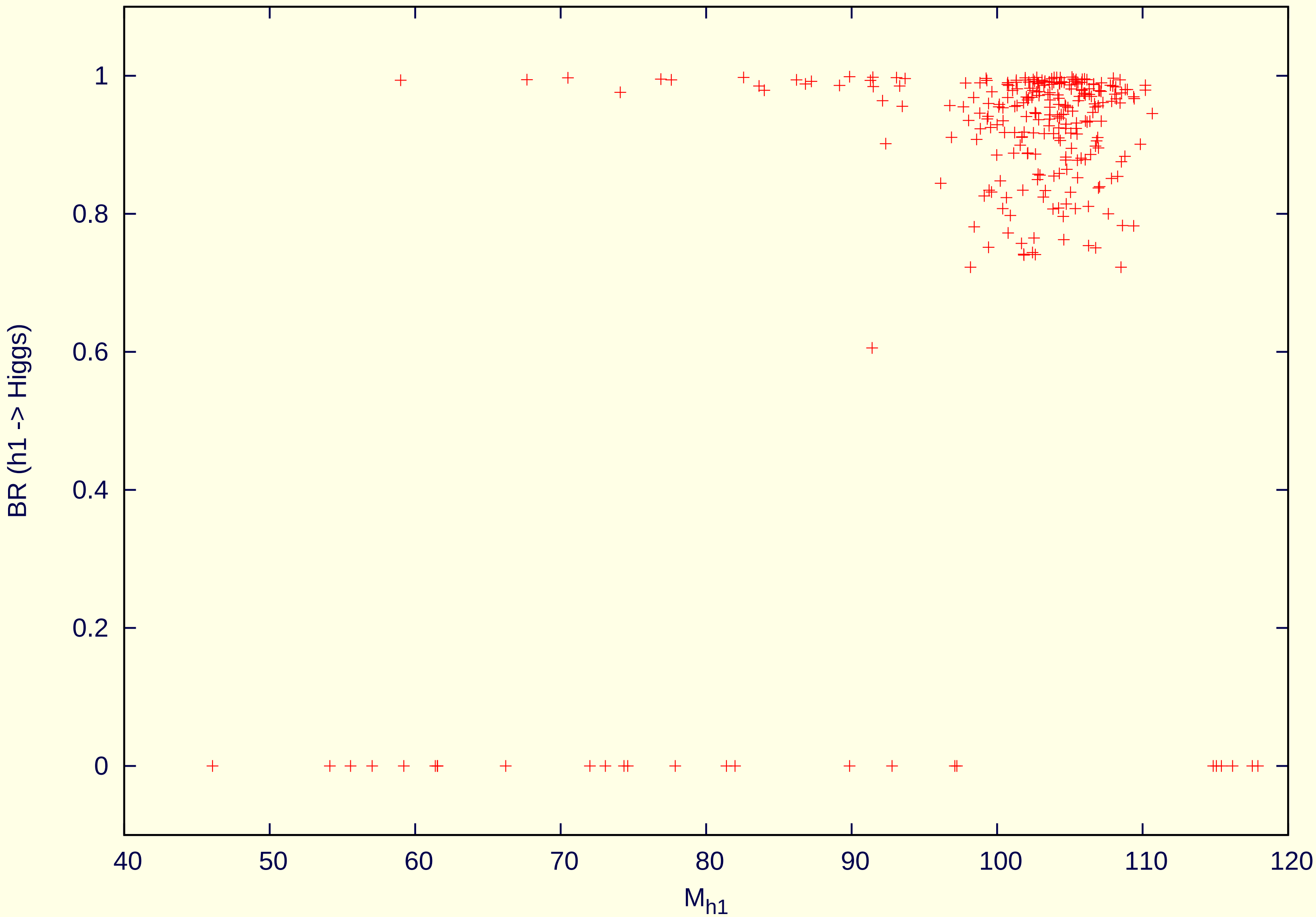

Figure 2: Scatter plot of $BR(h_1 \to a_1 a_1)$ vs. m_{h_1} for points with $v/T_c > 1$.

Baryogenesis favors $h_1 \to a_1 a_1$ scenarios!

NMHDECAY

We (Ellwanger, Hugonie, JFG [14]) have developed the NMSSM analogue of HDECAY. We provide two forms of the NMHDECAY program:

- **NMHDECAY_SLHA.f** — for study of one parameter point in the SLHA conventions for particle labeling etc. familiar to experimentalists;
- **NMHDECAY_SCAN.f** — designed for general phenomenological work including scanning over ranges of NMSSM parameters.

The programs, and associated data files, can be downloaded from the two web pages:

`http://www.th.u-psud.fr/NMHDECAY/nmhdecay.html`

`http://higgs.ucdavis.edu/nmhdecay/nmhdecay.html`

The web pages provide simplified descriptions of the programs and instructions on how to use them. The programs will be updated to include additional features and refinements in subsequent versions. We welcome comments with regard to improvements that users would find helpful.

Input files are `slhainp.dat` and `scaninp.dat`, respectively. They are simple!

```
#
#  Total number of points scanned
#
1000
#
#  Output format 0=short 1=long (not recommended for big scannings)
#
0
#
#  lambda
#
0.5
0.5
#
#  kappa
#
-0.15
-0.15
#
#  tan(beta)
#
3.5
3.5
#
#  mu
#
200.
200.
#
#  A_lambda
#
780.
780.
#
#  A_kappa
#
150.0
250.0
```

Table 1: Sample `scaninp.dat` file — 1st half for sample case #2.

```
#
#  Remaining soft terms (no scan)
#
mQ3=  1.D3
mU3=  1.D3
mD3=  1.D3
mL3=  1.D3
mE3=  1.D3
AU3=  1.5D3
AD3=  1.5D3
AE3=  1.5D3
mQ=   1.D3
mU=   1.D3
mD=   1.D3
mL=   1.D3
mE=   1.D3
M1=   5.D2
M2=   1.D3
M3=   3.D3
```

Table 2: The 2nd half of `scaninp.dat` file for sample case #2.

NMHDECAY performs the following tasks:

1. **It computes the masses and couplings of all physical states in the Higgs, chargino and neutralino sectors.**[1]

   Error messages are produced if a Higgs or squark mass squared is negative.

2. **It computes the branching ratios into two particle final states (including charginos and neutralinos — decays to squarks and sleptons will be implemented in a later release) of all Higgs particles.**

3. **It checks whether the Higgs masses and couplings violate any bounds from negative Higgs searches at LEP, including many quite unconventional channels that are relevant for the NMSSM Higgs sector.**

   It also checks the bound on the invisible Z width (possibly violated for light neutralinos).

[1] For the Higgses, we have included the leading two-loop effects, but neglected subleading two-loop contributions and subleading one-loop purely electroweak contributions. In MSSM limit, our Higgs masses agree to within a few GeV with HDECAY.

In addition, NMHDECAY checks the bounds on the lightest chargino and on neutralino pair production.

Corresponding warnings are produced in case any of these phenomenological constraints are violated.

4. It checks whether the running Yukawa couplings encounter a Landau singularity below the GUT scale.

   A warning is produced if this happens.

5. Finally, NMHDECAY checks whether the physical minimum (with all vevs non-zero) of the scalar potential is deeper than the local unphysical minima with vanishing $\langle H_u \rangle$ or $\langle H_d \rangle$.

   If this is not the case, a warning is produced.

- Below, I will discuss an example we employ to illustrate the use of these programs.

  It represents a scenario in which Higgs to Higgs decays make LHC Higgs detection very difficult.

  Other cases will be discussed.

Scenarios where LHC Higgs detection is hard

- **First, recall that normal MSSM Higgs detection at the LHC relies on:**

  1) $gg \to h/a \to \gamma\gamma$;
  2) associated Wh/a or $t\bar{t}h/a$ production with $\gamma\gamma\ell^{\pm}$ in the final state;
  3) associated $t\bar{t}h/a$ production with $h/a \to b\bar{b}$;
  4) associated $b\bar{b}h/a$ production with $h/a \to \tau^+\tau^-$;
  5) $gg \to h \to ZZ^{(*)} \to$ 4 leptons;
  6) $gg \to h \to WW^{(*)} \to \ell^+\ell^-\nu\bar{\nu}$;
  7) $WW \to h \to \tau^+\tau^-$;
  8) $WW \to h \to WW^{(*)}$.

  In supersymmetric models, it is also useful to include the mode

  9) $WW \to h \to invisible$.

  which, however, plays little role in the following. We also assume that $t \to H^{\pm}b$ will be observable for $m_{H^{\pm}} < 155~\mathrm{GeV}$ (could be raised).

- **We estimate the expected statistical significances at the LHC in all Higgs** boson detection modes 1) – 9) by rescaling results for the SM Higgs boson and/or the the MSSM h, H and/or A.

- $\boxed{\text{Scenarios for which LHC Higgs detection is ``easy'', for } L = 300\text{fb}^{-1}\text{!}}$

If Higgs decays to Higgs and/or SUSY are forbidden, then [26]: We can always detect at least one of the NMSSM Higgs bosons.

This was not the case [19] until the $t\bar{t}h \to t\bar{t}b\bar{b}$ mode [20, 21] (We have had the experimentalists extrapolate this beyond the usual SM mass range of interest.) and the WW fusion modes [22, 23, 24] were brought into play.

The point yielding the very lowest LHC statistical significance in an extensive scan over 10^9 points in parameter space had the following parameters:

$$\lambda = 0.0535; \quad \kappa = 0.0259; \quad \tan\beta = 5.42; \quad \mu_{\rm eff} = 145; \quad A_\lambda = -46 \text{ GeV}; \quad A_\kappa = -141 \text{ GeV}. \tag{28}$$

Properties of the Higgs bosons for this point are listed in table 3.

Other points with relatively weak LHC signals are similar in that:

1. the Higgs masses are closely spaced and below or at least not far above the WW/ZZ decay thresholds,

2. the CP-even Higgs bosons tend to share the WW/ZZ coupling strength (indicated by R_i in the table),
3. couplings to $b\bar{b}$ of all Higgs bosons (the b_i or b'_i in the table) are not very enhanced,
4. and couplings to gg (the g_i or g'_i in the table) are suppressed relative to the SM Higgs comparison.

The most visible process for this point was the $WW \to h_3 \to \tau^+\tau^-$ channel, but many other (notably $t\bar{t}h \to t\bar{t}b\bar{b}$) channels are also visible.

Overall, we have a quite robust LHC no-lose theorem for NMSSM parameters such that LEP constraints are passed and Higgs-to-Higgs decays are not allowed once full LHC luminosity is achieved.

It would be a good idea for the LHC experimentalists to check that one really can see the Higgs signals at our estimated levels for this worst case no-Higgs-to-Higgs point.

It would be a good idea to see what can the Tevatron do with such a point!

Table 3: Properties of the neutral NMSSM Higgs bosons for the most difficult no-Higgs-to-Higgs-decays LHC point. In the table, $R_i = g_{h_i VV}/g_{h_{SM} VV}$, $t_i = g_{h_i t\bar t}/g_{h_{SM} t\bar t}$, $b_i = g_{h_i b\bar b}/g_{h_{SM} b\bar b}$ and $g_i = g_{h_i gg}/g_{h_{SM} gg}$ for $m_{h_{SM}} = m_{h_i}$. Similarly, t'_i and b'_i are the $i\gamma_5$ couplings of a_i to $t\bar t$ and $b\bar b$ normalized relative to the scalar $t\bar t$ and $b\bar b$ SM Higgs couplings and g'_i is the $a_i gg$ $\epsilon \times \epsilon'$ coupling relative to the $\epsilon \cdot \epsilon'$ coupling of the SM Higgs.

Higgs	h_1	h_2	h_3	a_1	a_2
Mass (GeV)	94	113	147	133	173
R_i	-0.440	-0.743	-0.505	0	0
t_i or t'_i	-0.421	-0.647	-0.662	-0.183	0.026
b_i or b'_i	-0.993	-3.55	4.10	-5.37	0.757
g_i or g'_i	0.470	0.554	0.435	0.139	0.021
$B(h_i\ or\ a_i \to b\bar b)$	0.902	0.908	0.870	0.911	0.903
$B(h_i\ or\ a_i \to \tau^+\tau^-)$	0.081	0.085	0.086	0.088	0.095
Chan. 1) $S/\sqrt{B}$	0.00	0.20	0.26	0.00	0.00
Chan. 2) $S/\sqrt{B}$	0.83	0.76	0.22	0.00	0.00
Chan. 3) $S/\sqrt{B}$	3.03	6.28	5.64	5.64	0.00
Chan. 4) $S/\sqrt{B}$	0.00	0.88	3.24	3.24	0.04
Chan. 5) $S/\sqrt{B}$	0.00	0.12	1.59	$-$	$-$
Chan. 6) $S/\sqrt{B}$	0.00	0.00	1.26	$-$	$-$
Chan. 7) $S/\sqrt{B}$	0.00	6.88	6.96	$-$	$-$
Chan. 8) $S/\sqrt{B}$	0.00	0.17	0.44	$-$	$-$
All-channel $S/\sqrt{B}$	3.14	9.39	9.75	6.50	0.04

- **The difficult scenarios: Higgs to Higgs (or SUSY) decays**

  The importance of Higgs to Higgs decays was first realized at Snowmass 1996 (JFG, Haber, Moroi [19]) and was later elaborated on in [25]. Detailed NMSSM scenarios were first studied in [26, 27].

  We have shown that (for relatively heavy squarks and gauginos) all scenarios of this type for which discovery is not possible in modes 1) – 9) are such that there is a SM-like Higgs h_H which decays to a pair of lighter Higgs, $h_L h_L$.

  In general, the h_L decays to $b\bar{b}$ and $\tau^+\tau^-$ (if $m_{h_L} > 2m_b$) or to jj and $\tau^+\tau^-$ (if $2m_\tau < m_{h_L} < 2m_b$) or, as unfortunately still possible, to jj if $m_{h_L} < 2m_\tau$.

  In the first two cases, a possibly viable LHC signal then comes [26, 27] from $WW \to h_H \to h_L h_L \to jj\tau^+\tau^-$ in the form of a bump in the $M_{jj\tau^+\tau^-}$ reconstructed mass distribution. It is not a wonderful signal, but it is a signal.

  For most such cases, h_L is actually the lightest CP-odd scalar a_1 and h_H is the lightest or 2nd lightest CP-even scalar, h_1 or h_2.

Experimentalists should work hard to see if our crude estimates that there would be an observable signal at the LHC will survive reality.

- As regards the cases where $m_{a_1} < 2m_\tau \Rightarrow a_1 \to c\bar{c}, s\bar{s}, gg$, these can often evade LEP limits (but we are pushing the LEP people for improvements).

  It will be very difficult extract a signal in these cases where neither b nor τ tagging is relevant. The only hope would be jet counting, but QCD backgrounds are probably enormous.

  Since the $b\bar{b}$ coupling of these very light a_1's is not enhanced significantly (typically), there are no reliable exclusions coming from Υ or $B_{s,d}$ decays. We believe there is simply too much model dependence in the theory for such decays, although we would be happy to be persuaded otherwise.

- There are also cases in which $h_H = h_2$ and $h_L = h_1$, $m_{h_1} > 2m_b$, but yet $h_1 \to c\bar{c}, gg$ decays are completely dominant — parameters are chosen near a special region where the h_1 decouples from leptons and down-type quarks.

  Again, it is very hard to imagine a technique for extracting a signal at the LHC.

- **The basic question: Can the Tevatron be sensitive to the Higgs-to-Higgs decay scenarios?**

  To assess this, we go through some benchmark points that will appear in a forthcoming paper (JFG, Ellwanger, Hugonie, Moretti).

Some Benchmark Points

Generically speaking, the NMSSM is capable of producing a large variety of Higgs phenomenologies. Here, we wish to delineate the kinds of scenarios that have not been excluded by LEP but might have a significant chance of allowing Higgs discovery at the Tevatron. Primary among these appear to be the scenarios in which there is a somewhat light SM-like Higgs boson that decays in unconventional fashion to two still lighter Higgs bosons, most commonly in the CP-conserving framework that we focus on here, a pair of the lightest CP-odd states. Thus, we focus on the $h \to aa$ situations that can arise in the NMSSM. These are also those favored by finetuning and electroweak baryogenesis.

The $h \to aa$ decays lead to the following final states:

(i) 4 b's, 2b's + 2τ's, or 4τ's, when $m_a > 2m_b$;

(ii) 4 c's, 2c's + 2τ's, or 4τ's, when $2m_\tau < m_a < 2m_b$;

(iii) 4c's, 2c's + 2 jets, or 4 jets, when $2m_c < m_a < 2m_\tau$;

(iv) or 4 jets, when $m_a < 2m_c$. Here, jet = s or g.

There are only a limited number of LEP limits that can be applied in these cases.

- In case (i) above, the best limits are certainly those recently extracted specifically for the $Zh \to Zaa \to Zb\bar{b}b\bar{b}$ final state. The 95% CL contours for $C^2 = [g^2_{Zh}/[g^2_{Zh}]_{SM}] \times Br(h \to aa) \times [BR(a \to b\bar{b})]^2$, for various values of m_a, are shown in Fig. 3.

  We are not aware of any limits yet extracted for the $Zh \to Zaa \to Zb\bar{b}\tau^+\tau^-$ or $Zh \to Zaa \to Z\tau^+\tau^-\tau^+\tau^-$ final states. However, we understand that some are forthcoming.

- The $Z + 4b$ final state limit is only superior to the $Zh \to Z + hadrons$ final state independent limit, plotted in Fig. 3 and, in more detail, in Fig. 4 for $m_h \gtrsim 45~\mathrm{GeV}$. The Fig. 4 limit is for $C^2 = [g^2_{Zh}/[g^2_{Zh}]_{SM}] \times BR(h \to aa) \times [BR(a \to \textbf{hadrons})]^2$, where the $hadrons$ refers to a state with any number of jets.

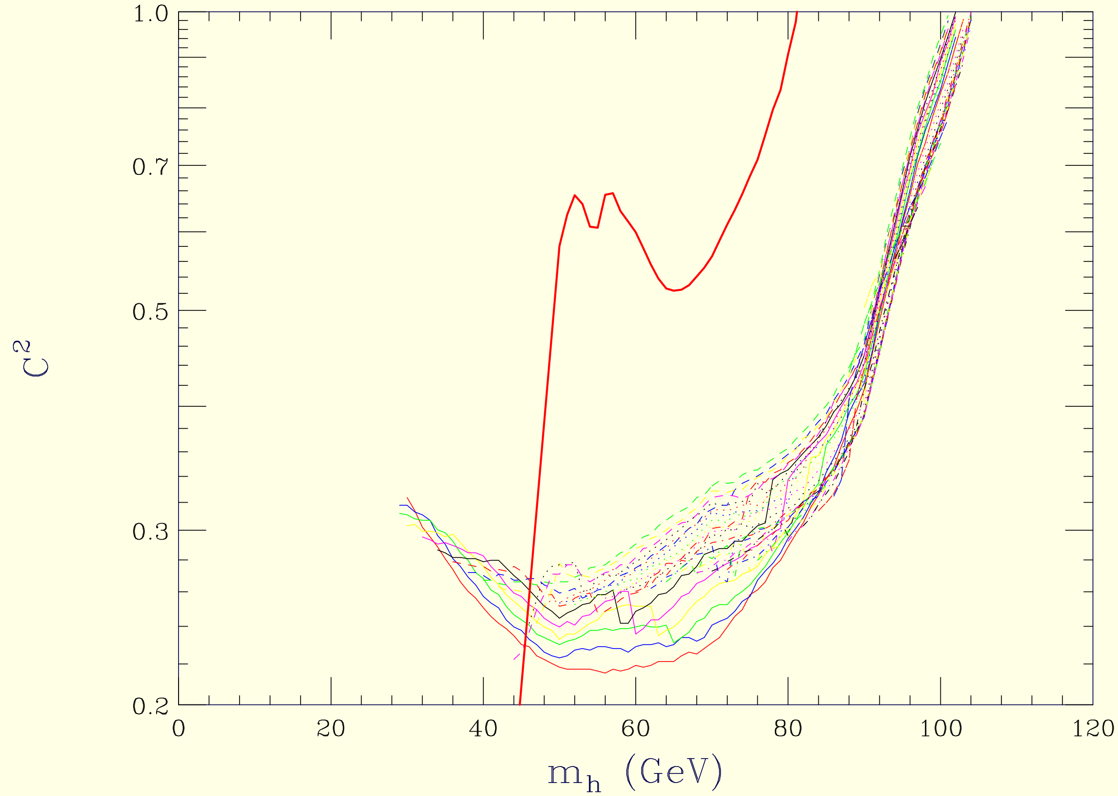

Figure 3: Plot of the 95% CL limits on $C^2 = [g^2_{Zh}/[g^2_{Zh}]_{SM}] \times BR(h \to aa) \times [BR(a \to b\bar{b})]^2$. The different curves are for different m_a values: solid lines are for 12, 13, 14, 15, 16 and 17 GeV in order of red, blue, green, yellow, magenta, black; dotted lines are for 18, 19, 20, 21, 22 and 23 in same color order; dotted lines are for 24, 25, 26, 27, 28 and 29 in same color order; dotdash lines are for 30, 31, 32, 33, 34, and 35 in same color order; long-dash lines are for 36, 37, 38, 39, 40 and 41 in same color order; and dot-dot-dash lines are for 42, 43, 44, 45 46 and 47 in same color order. The thick solid red line is the line of Fig. 4 for this same mass region.

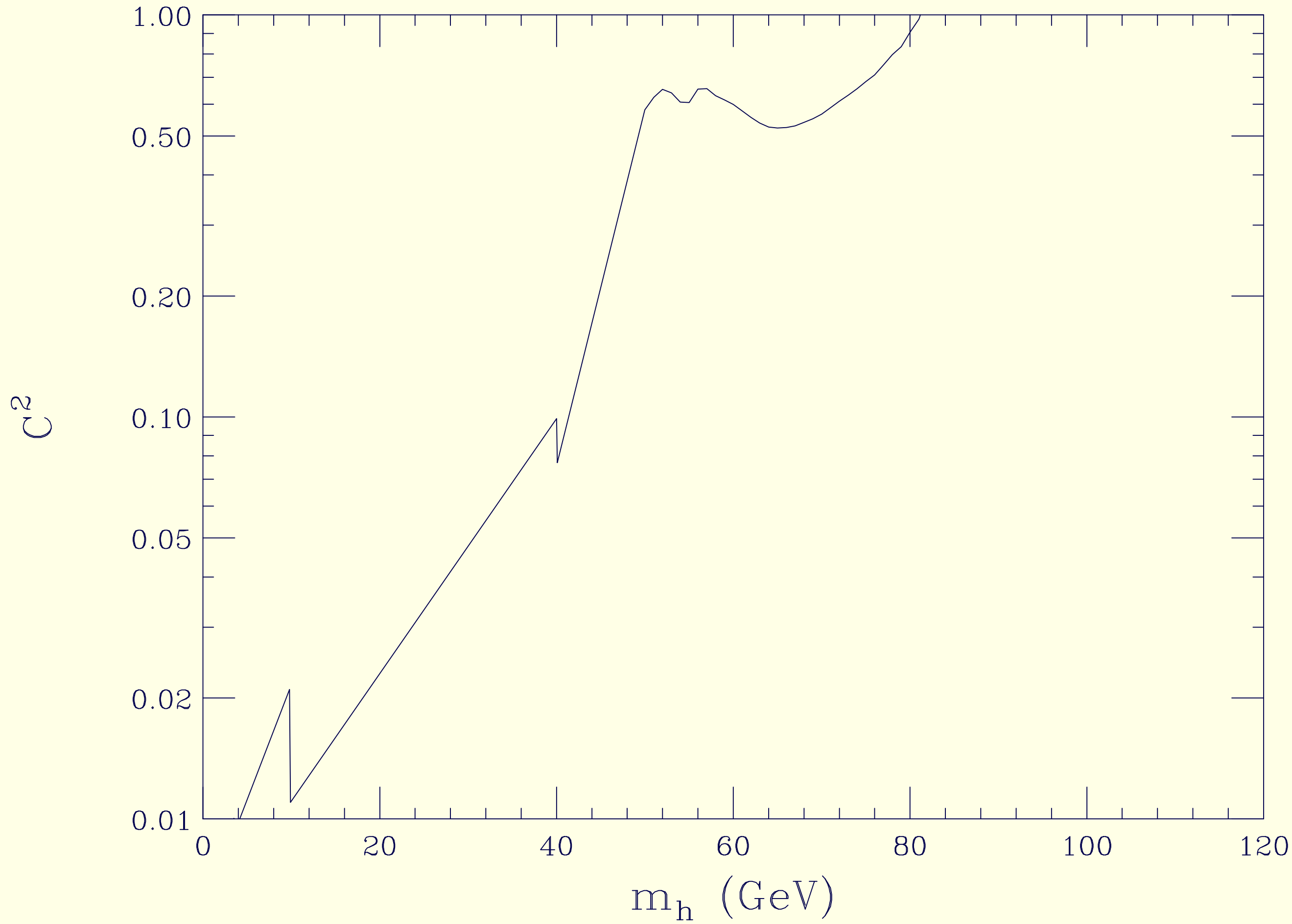

Figure 4: **Plot of the 95% CL limit on $C^2 = [g^2_{Zh}/[g^2_{Zh}]_{SM}] \times BR(h \to \text{hadrons})$, where h is only assumed to decay to hadrons, not any specific number of jets.**

- In cases (ii), (iii), and (iv), only the $Zh \to Z + hadrons$ limits remain potentially useful.

- However, some specific limits have been obtained for $m_h \in [40, 90]~\mathrm{GeV}$ with $m_a < 2m_b$.

  So far these are only available as upper bound plots in the m_h, m_a parameter space of the regions in which the $Zh \to Zaa \to Z + F$ signals are excluded at 95% CL for values of $C^2 = 0.2$, 0.4, 0.5, 0.6, 0.8 and 1, where $C^2 = [g^2_{Zh}/[g^2_{Zh}]_{SM}] \times BR(aa \to F)$, where F stands for any of the relevant final states, such as $F = \tau^+\tau^-\tau^+\tau^-$, $c\overline{c}\tau^+\tau^-$, $c\overline{c}c\overline{c}$, $\ldots$.

- Typically, for $2m_\tau < m_a < 2m_b$ one finds $BR(a \to \tau^+\tau^-) \sim 0.8$ and $BR(a \to c\overline{c}) \sim 0.2$, implying dominance of the $\tau^+\tau^-\tau^+\tau^-$, $\tau^+\tau^-c\overline{c}$ and $c\overline{c}c\overline{c}$ final states, with other final states being negligible.

- For $2m_c < m_a < 2m_\tau$, the $a \to c\overline{c}$ decay is dominant and the $Z + c\overline{c}c\overline{c}$ final state will be of primary interest.

- The relevant plots appear in Figs. 5-10. For $m_h < 40~\mathrm{GeV}$, one must turn to Fig. 4 as the only available limit.

  A plot like Fig. 4 and ones like Figs. 5 and 6 appear on page 10 and page 12, respectively, of Boonekamp's talk at CPNSH.

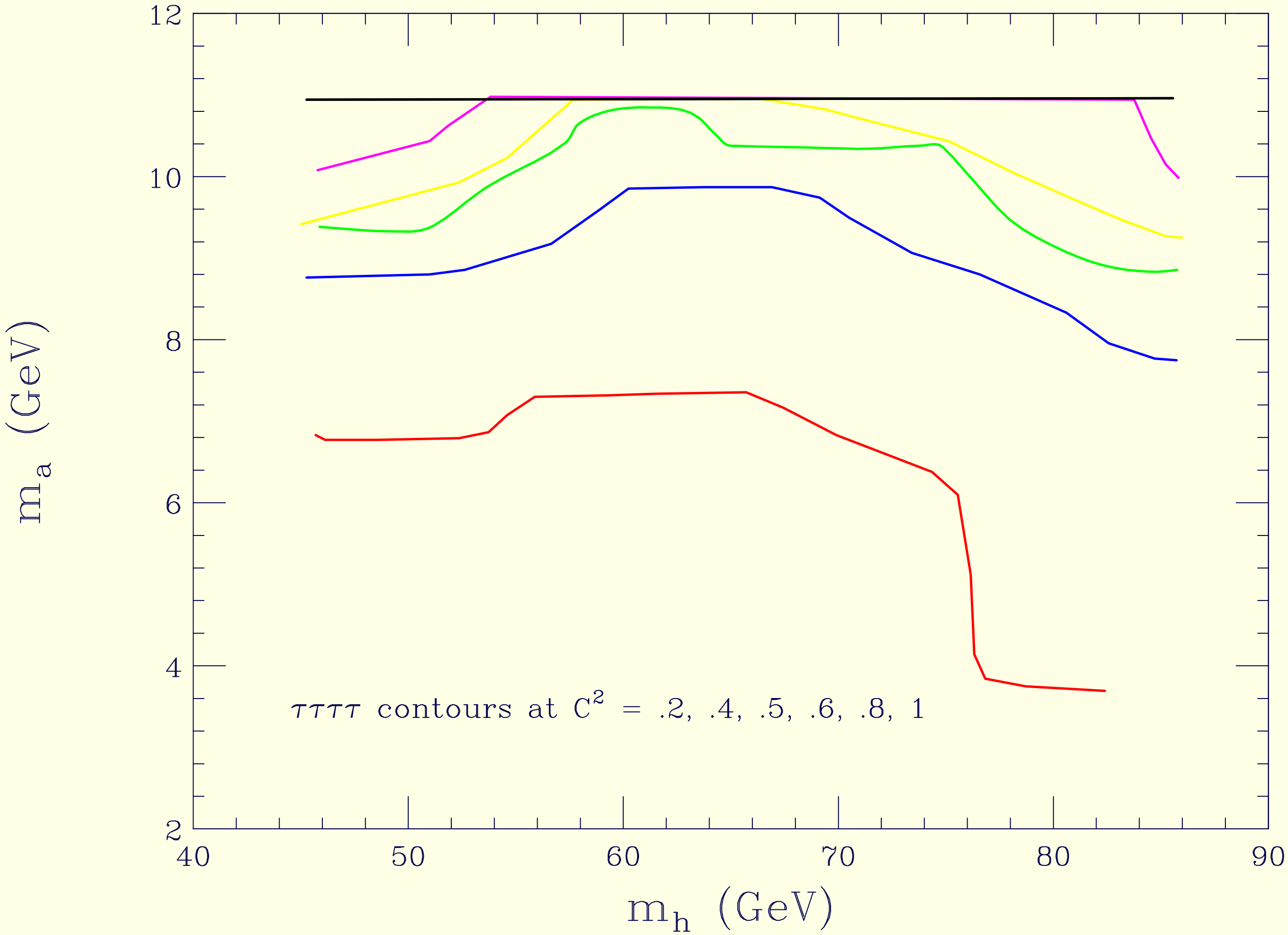

Figure 5: **Contours of limits on** $C^2 = [g^2_{Zh}/[g^2_{Zh}]_{SM}] \times BR(h \to aa) \times [BR(a \to \tau^+\tau^-)]^2$ **at** $C^2 = 0.2$, 0.4, 0.5, 0.6, 0.8 **and** 1 **(red, blue, green, yellow, magenta, and black, respectively). For example, if** $C^2 > 0.2$**, then the region below the** $C^2 = 0.2$ **contour is excluded at 95% CL.**

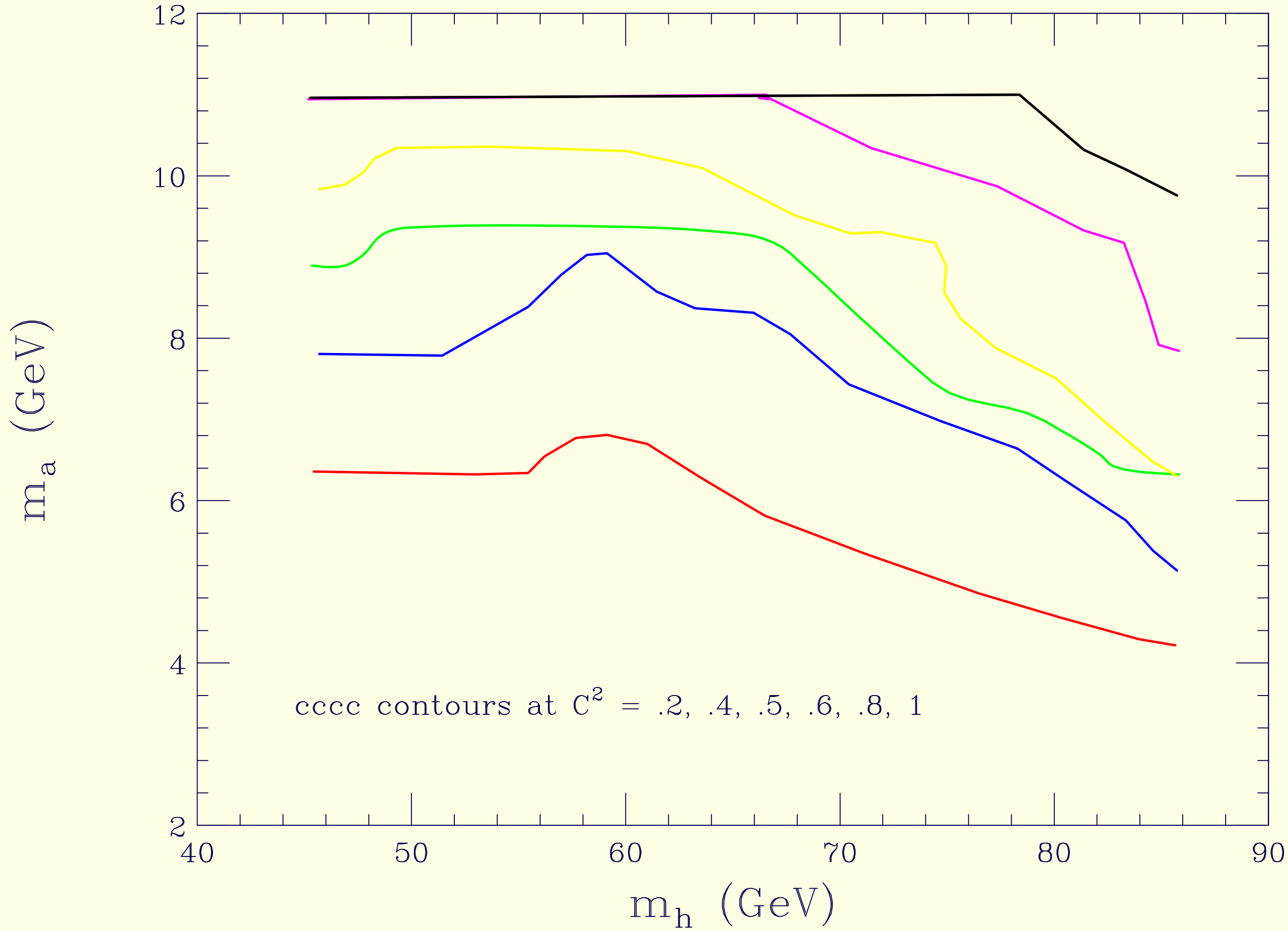

Figure 6: **Contours of limits on** $C^2 = [g^2_{Zh}/[g^2_{Zh}]_{SM}] \times BR(h \to aa) \times [BR(a \to c\overline{c})]^2$ **at** $C^2 = 0.2$**,** 0.4**,** 0.5**,** 0.6**,** 0.8 **and** 1 **(red, blue, green, yellow, magenta, and black, respectively). For example, if** $C^2 > 0.2$**, then the region below the** $C^2 = 0.2$ **contour is excluded at 95% CL.**

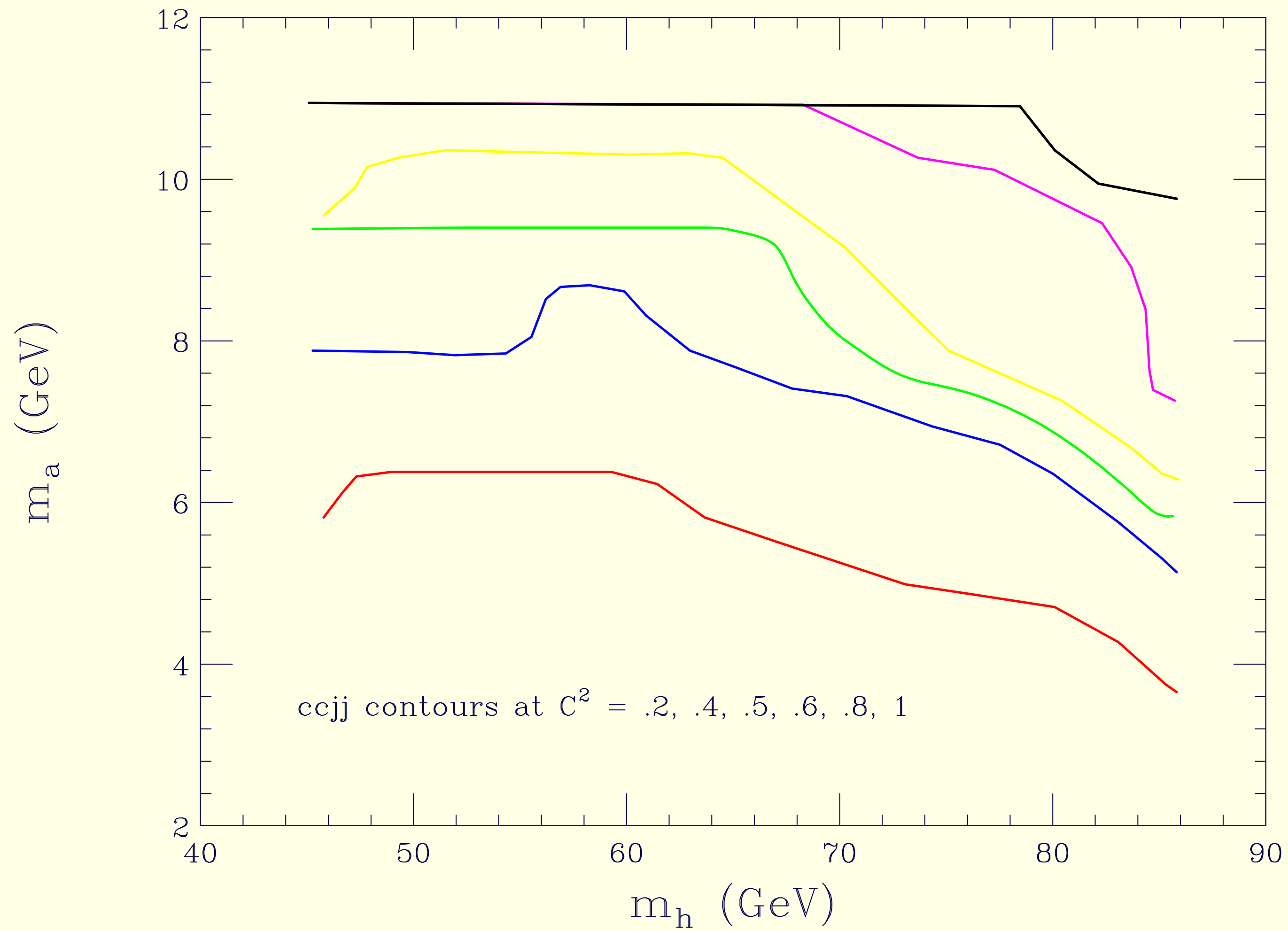

Figure 7: **Contours of limits on**
$C^2 = [g^2_{Zh}/[g^2_{Zh}]_{SM}] \times BR(h \to aa) \times \; 2BR(a \to c\bar{c}) \; BR(a \to s\bar{s} + gg)$
at $C^2 = 0.2$, 0.4, 0.5, 0.6, 0.8 and 1 (red, blue, green, yellow, magenta, and black, respectively). For example, if $C^2 > 0.2$, then the region below the $C^2 = 0.2$ contour is excluded at 95% CL.

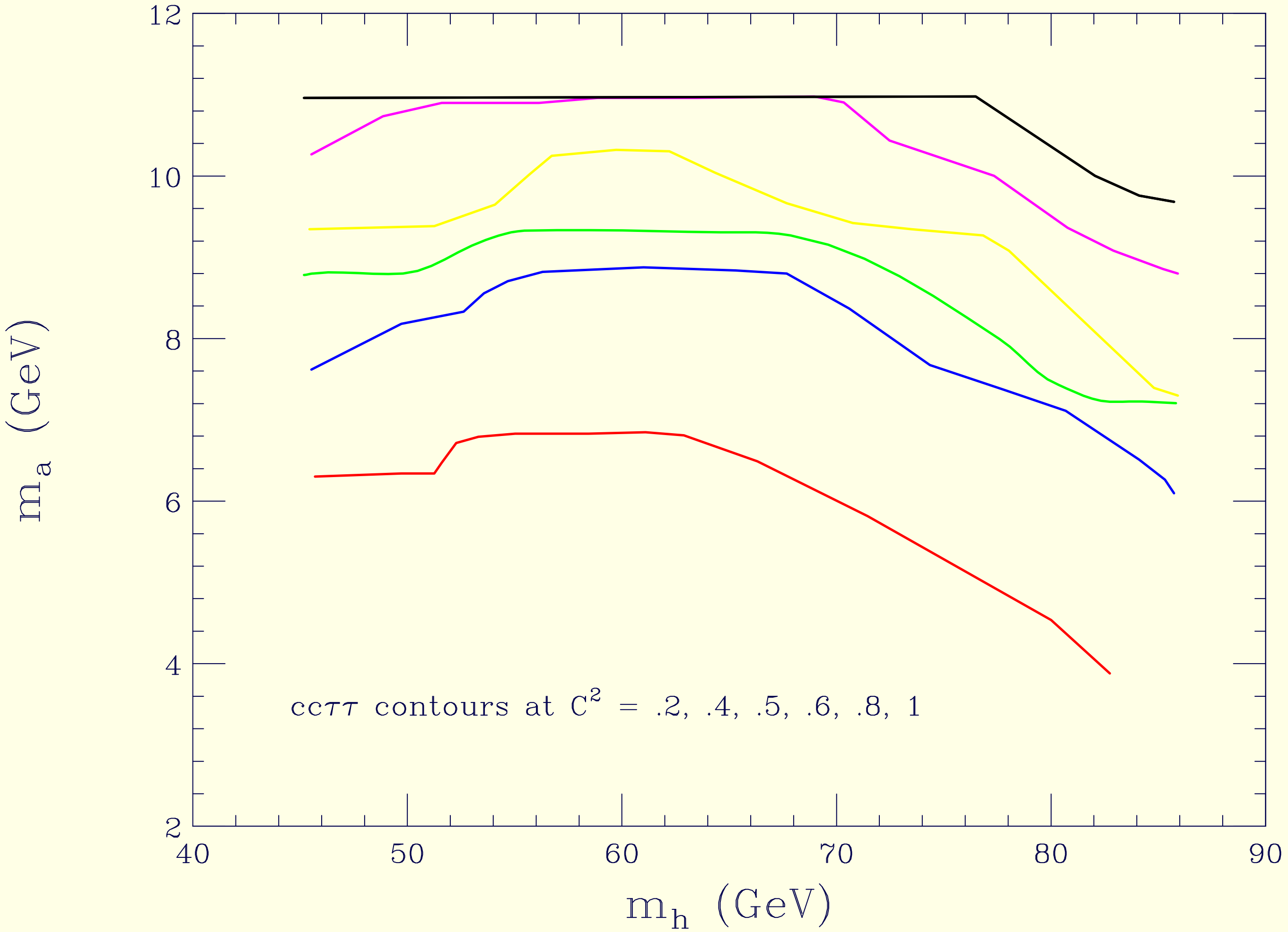

Figure 8: **Contours of limits on**
$C^2 = [g^2_{Zh}/[g^2_{Zh}]_{SM}] \times BR(h \to aa) \times \ 2BR(a \to c\overline{c}) \ BR(a \to \tau^+\tau^-)$
at $C^2 = 0.2$, 0.4, 0.5, 0.6, 0.8 and 1 (red, blue, green, yellow, magenta, and black, respectively). For example, if $C^2 > 0.2$, then the region below the $C^2 = 0.2$ contour is excluded at 95% CL.

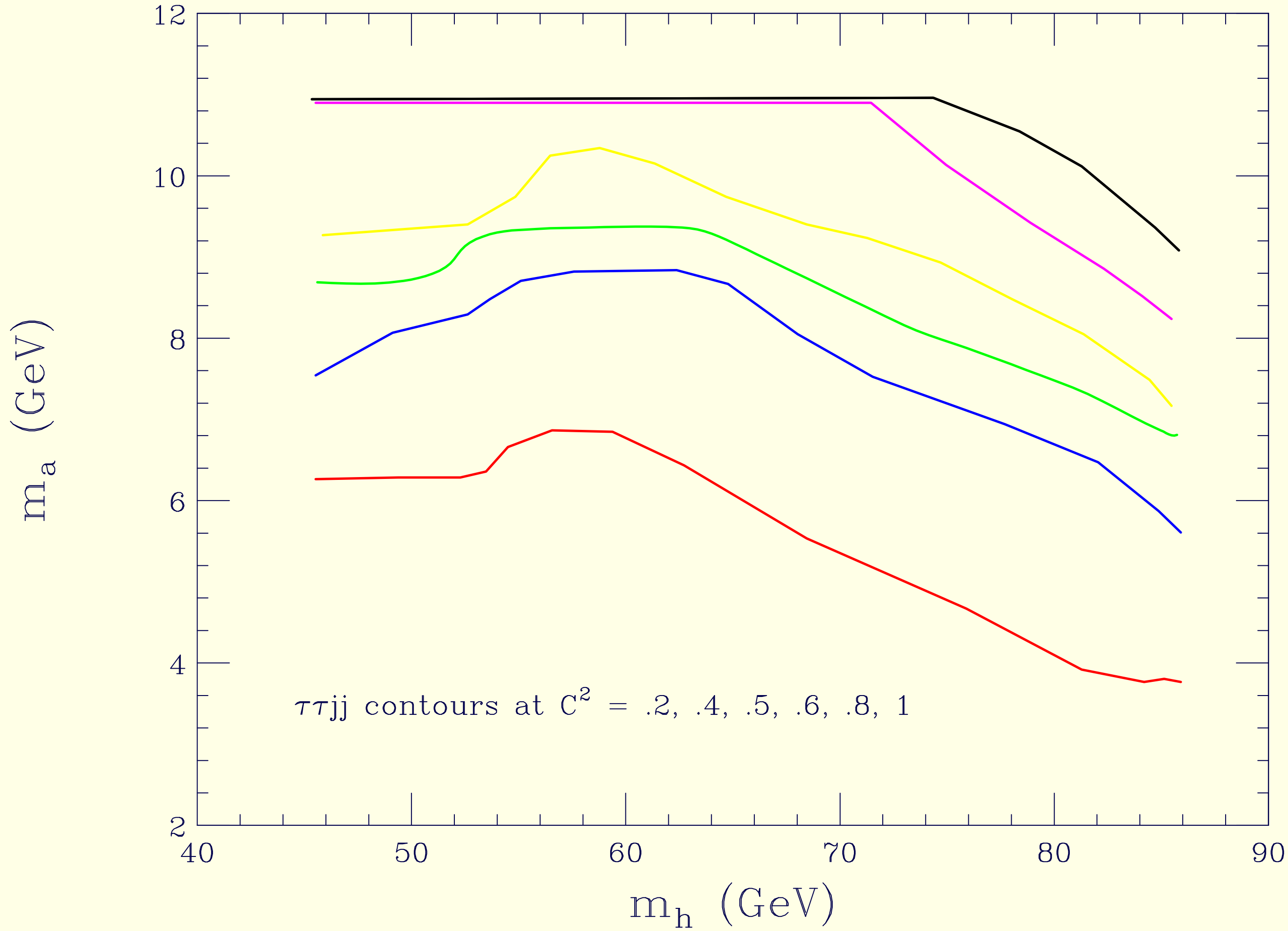

Figure 9: Contours of limits on
$C^2 = [g^2_{Zh}/[g^2_{Zh}]_{SM}] \times BR(h \to aa) \times 2\, BR(a \to \tau^+\tau^-) BR(a \to s\overline{s} + gg)$
at $C^2 = 0.2$, 0.4, 0.5, 0.6, 0.8 and 1 (red, blue, green, yellow, magenta, and black, respectively). For example, if $C^2 > 0.2$, then the region below the $C^2 = 0.2$ contour is excluded at 95% CL.

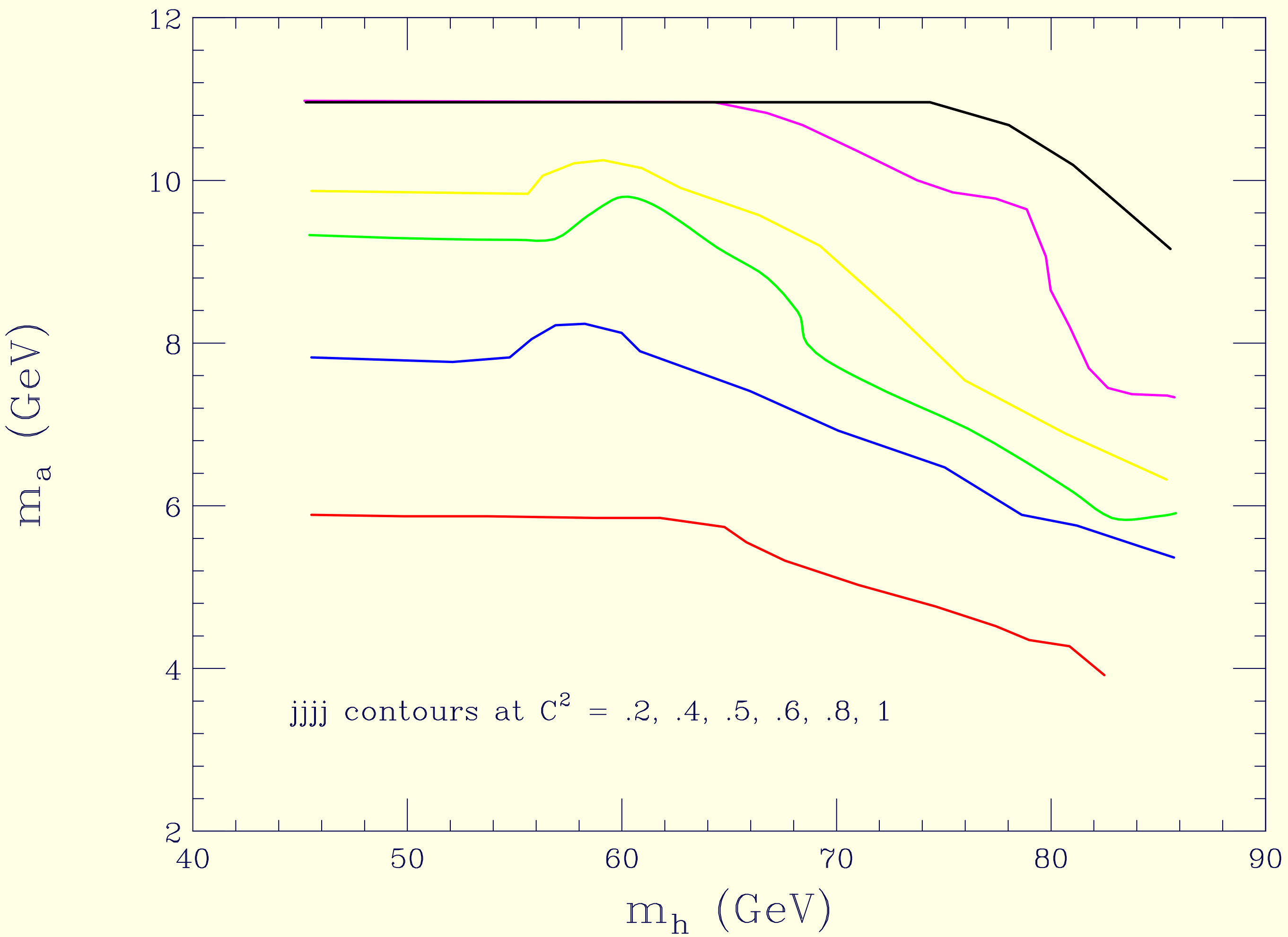

Figure 10: **Contours of limits on**
$$C^2 = [g^2_{Zh}/[g^2_{Zh}]_{SM}] \times BR(h \to aa) \times [BR(a \to s\bar{s} + gg)]^2$$
at $C^2 = 0.2$, 0.4, 0.5, 0.6, 0.8 and 1 (red, blue, green, yellow, magenta, and black, respectively). For example, if $C^2 > 0.2$, then the region below the $C^2 = 0.2$ contour is excluded at 95% CL.

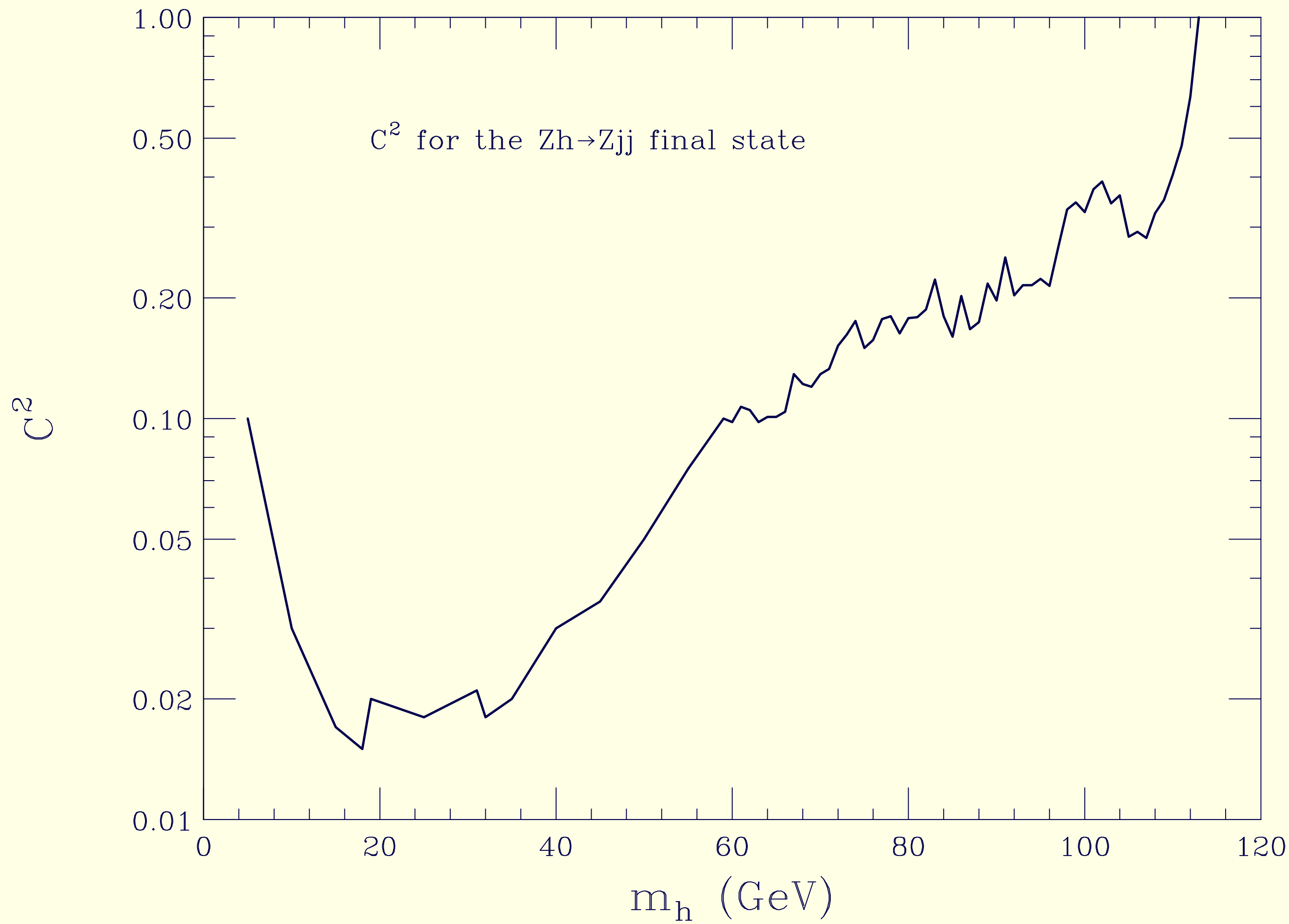

Figure 11: 95% CL upper limit on $C^2 = [g^2_{Zh}/[g^2_{Zh}]_{SM}] \times BR(h \to jj)$ **from LEP analyzes.**

Tevatron Implications of LHC scenarios

All the parameter space points listed below escape the LEP limits for one reason or another, as sketched below.

In the tables,

- $R_i = g_{h_i VV}/g_{h_{SM} VV}$,
- $t_i = g_{h_i t\bar{t}}/g_{h_{SM} t\bar{t}}$,
- $b_i = g_{h_i b\bar{b}}/g_{h_{SM} b\bar{b}}$
- and $g_i = g_{h_i gg}/g_{h_{SM} gg}$

for $m_{h_{SM}} = m_{h_i}$.

Similarly,

- t'_i and b'_i are the $i\gamma_5$ couplings of a_i to $t\bar{t}$ and $b\bar{b}$ normalized relative to the scalar $t\bar{t}$ and $b\bar{b}$ SM Higgs couplings
- and g'_i is the $a_i gg$ $\epsilon \times \epsilon'$ coupling relative to the $\epsilon \cdot \epsilon'$ coupling of the SM Higgs.

Point Number	1	2	3	4	5
Bare Parameters					
λ	0.390	0.220	0.400	0.340	0.220
κ	$-.280$	$-.100$	$-.350$	$-.440$	0.590
$\tan\beta$	24.00	5.00	15.00	2.90	7.80
$\mu_{\rm eff}$	-140.0	-520.0	-160.0	120.0	530.0
A_λ	-350.0	-580.0	-580.0	450.0	-920.0
A_κ	-5.8	-2.8	-8.7	44.0	-2.1
CP-even Higgs Boson Masses and Couplings					
m_{h_1} (GeV)	79.2	90.4	99.7	109.8	119.5
R_1	0.893	0.986	0.966	-0.994	-1.000
t_1	0.893	0.986	0.966	-0.979	-1.000
b_1	0.776	1.003	0.901	-1.117	-1.010
g_1	0.900	0.985	0.969	0.974	0.999
$B(h_1 \to b\overline{b})$	0.035	0.076	0.024	0.003	0.009
$B(h_1 \to \tau^+\tau^-)$	0.003	0.007	0.002	0.000	0.001
$B(h_1 \to a_1 a_1)$	0.958	0.910	0.970	0.997	0.988
m_{h_2} (GeV)	221.1	478.9	287.9	304.1	1430.6
R_2	-0.451	-0.165	-0.260	0.084	-0.001
t_2	-0.450	-0.164	-0.259	-0.016	-0.129
b_2	-0.731	-0.193	-0.570	0.922	7.798
g_2	0.446	0.164	0.256	0.022	0.121
$B(h_2 \to b\overline{b})$	0.002	0.000	0.001	0.004	0.154
$B(h_2 \to \tau^+\tau^-)$	0.000	0.000	0.000	0.000	0.022
$B(h_2 \to W^+W^- + ZZ)$	0.417	0.569	0.338	0.051	0.000
$B(h_2 \to a_1 a_1)$	0.256	0.041	0.438	0.590	0.003
$B(h_2 \to h_1 h_1)$	0.324	0.247	0.214	0.013	0.001

Point Number	1	2	3	4	5
CP-odd Higgs Boson Masses and Couplings					
m_{a_1} (GeV)	8.4	9.8	20.4	40.5	31.5
t_1'	-0.002	-0.009	-0.004	0.128	-0.009
b_1'	-1.067	-0.217	-0.846	1.074	-0.533
g_1'	0.757	0.153	0.481	0.242	0.190
$B(a_1 \to b\bar{b})$	0.000	0.000	0.938	0.928	0.932
$B(a_1 \to \tau^+\tau^-)$	0.800	0.830	0.058	0.069	0.065
$B(a_1 \to c\bar{c} + s\bar{s} + gg)$	0.197	0.167	0.004	0.002	0.003

Table 4: Properties of selected scenarios for which Higgs detection at a hadron collider must rely on the $h_{1,2} \to a_1 a_1 \to jj\tau^+\tau^-$ or $h_2 \to h_1 h_1 \to jj\tau^+\tau^-$ modes, where $jj = b\bar{b}$ in many cases. The quantities R_i, t_i, b_i, g_i, t_i', b_i' and g_i' are discussed in the text. Important absolute branching ratios are also displayed.

Point Number	6	7	8	9
Bare Parameters				
λ	0.630	0.520	0.670	0.560
κ	0.280	0.190	0.200	0.100
$\tan\beta$	2.70	8.40	4.10	2.50
$\mu_{\rm eff}$	−430.0	135.0	−200.0	−180.0
A_λ	−925.0	680.0	−600.0	−440.0
A_κ	−17.5	12.0	−30.0	172.0
CP-even Higgs Boson Masses and Couplings				
m_{h_1} (GeV)	129.7	69.5	96.7	39.8
R_1	−1.000	−0.566	0.694	−0.001
t_1	−0.999	−0.574	0.717	0.055
b_1	−1.004	−0.006	0.310	−0.352
g_1	0.999	0.613	0.737	0.151
$B(h_1 \to b\overline{b})$	0.005	0.008	0.007	0.926
$B(h_1 \to \tau^+\tau^-)$	0.000	0.000	0.001	0.071
$B(h_1 \to a_1 a_1)$	0.991	0.797	0.988	0.000
m_{h_2} (GeV)	386.3	140.0	149.8	125.0
R_2	−0.011	−0.825	−0.719	−1.000
t_2	−0.041	−0.819	−0.697	−0.996
b_2	0.207	−1.229	−1.098	−1.027
g_2	0.041	0.807	0.687	0.995
$B(h_2 \to b\overline{b})$	0.001	0.021	0.010	0.056
$B(h_2 \to \tau^+\tau^-)$	0.000	0.002	0.001	0.005
$B(h_2 \to W^+W^- + ZZ)$	0.004	0.013	0.016	0.016
$B(h_2 \to a_1 a_1)$	0.986	0.812	0.972	0.000
$B(h_2 \to h_1 h_1)$	0.000	0.150	0.000	0.915

Point Number	6	7	8	9
CP-odd Higgs Boson Masses and Couplings				
m_{a_1} (GeV)	50.3	32.9	45.0	144.3
t'_1	-0.015	0.007	-0.024	-0.064
b'_1	-0.109	0.527	-0.401	-0.402
g'_1	0.018	0.177	0.076	0.058
$B(a_1 \to b\bar{b})$	0.924	0.931	0.927	0.855
$B(a_1 \to \tau^+\tau^-)$	0.073	0.066	0.071	0.083
m_{a_2} (GeV)	1200.0	904.4	750.2	495.5
$m_{h^\pm}$ (GeV)	1196.9	901.8	742.3	486.8

Table 5: Four additional scenarios for which Higgs discovery would need sensitivity to the $h \to a_1 a_1 \to jj\tau^+\tau^-$ ($h = h_1$ or h_2) or $h_2 \to h_1 h_1 \to jj\tau^+\tau^-$ modes, with $jj = b\bar{b}$ in many cases. Notations as in table 4.

Discussion of points 1 to 9: $a_1 \to b\bar{b}$ decays present

- **Point 1** provides a useful first example.

  Since $m_{h_1^0} \sim 79~\mathrm{GeV}$ is rather low, and since the gg coupling to h_1 is about 0.9 times SM strength, the Tevatron should have a a reasonable production rate in the gg fusion channel.

  In this case, $h_1 \to a_1 a_1$ decay completely dominates and since $m_{a_1} \sim 8.4~\mathrm{GeV}$, $a_1 a_1 \to \tau^+\tau^-$ is the relevant channel.

  This point escapes the LEP limits by virtue of the unusual $h_1 \to a_1 a_1 \to \tau^+\tau^-\tau^+\tau^-$ decay which avoids the constraints of both Fig. 3 and 4 by virtue of the fact that the final state is dominated by leptons or unexpectedly soft jets.

  Meanwhile $C^2(\tau^+\tau^-\tau^+\tau^-) = [g^2_{Zh_1}/g^2_{Zh_{\mathrm{SM}}}] \times BR(h_1 \to a_1 a_1) \times [BR(a_1 \to \tau^+\tau^-]^2 \sim 0.49$ just barely avoids being eliminated by the $C^2 = 0.4$ contour which excludes only $m_{a_1} \lesssim 8.3~\mathrm{GeV}$ at $m_{h_1^0} = 79~\mathrm{GeV}$, and is not subject to elimination by the $C^2 = 0.5$ contour (which would exclude $C^2 \geq 0.5$ for $m_{a_1} \leq 9.2$ for $m_{h_1^0} = 79~\mathrm{GeV}$).

Better analysis of this specific configuration by the LEP experimentalists might well exclude this point, but we could easily shift parameters slightly.

At the Tevatron, the gg production rate for the h_1 will be $g_1^2 = 0.9^2 = 0.81$ of the SM rate.

Is it possible to extract the 4τ signal for the h_1 in the gg fusion mode?

Of course, we should also note that the WW fusion coupling squared ($R_1^2 \sim 0.893^2 \sim 0.8$) is close to SM-like and one can tag forward and backward jets.

Wh associated production could also be considered. It provides a trigger and some handle on backgrounds as compared to gg fusion.

However, the lower masses of the Higgs boson being considered here and at subsequent parameter space points only gives a factor of $\sim 2 \div 4$ increase relative to $m_h \gtrsim 115~\mathrm{GeV}$.

The main question is whether backgrounds are lower for this kind of scenario as compared to the LHC situation with much higher Higgs cross section, but also much higher backgrounds.

Cross Section Reality Check

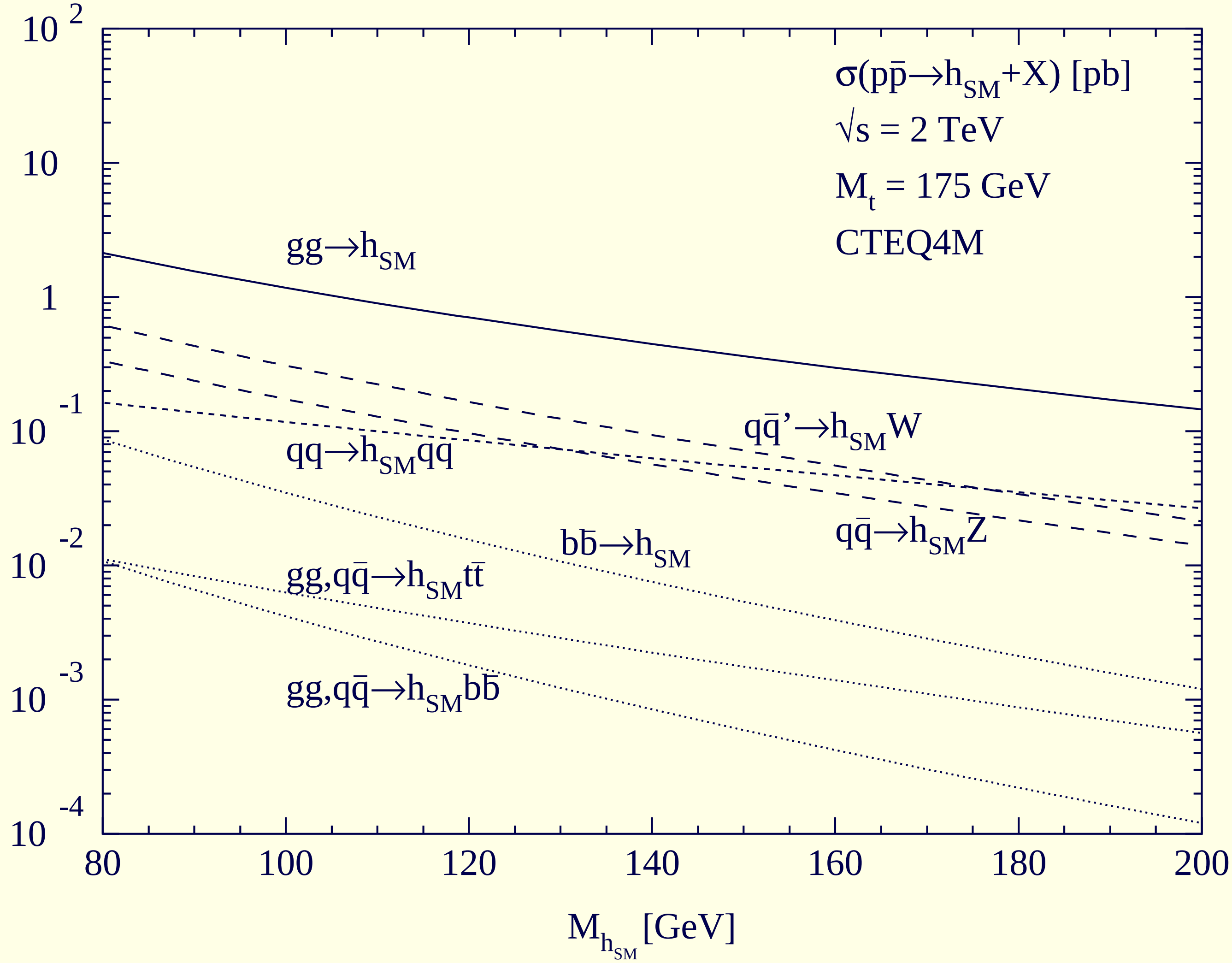

Figure 12: **Various cross sections at the Tevatron for a SM Higgs boson. Note the small size of WW fusion at low m_h. Better is Wh associated production,**

- **Point 2** provides a similar example at somewhat higher $m_{h_1^0} = 90.4$ GeV and similar $m_{a_1} \sim 9.8$ GeV.

  In particular, even though $C^2(\tau^+\tau^-\tau^+\tau^-) \sim 0.61$ in this case, the m_{a_1} value is sufficiently large that even an extension of the 0.6 LEP contour of Fig. 5 to $m_{h_1^0} \sim 90.4$ GeV would be unlikely to exclude this point.

  Meanwhile, the gg fusion and WW fusion production rates are $0.97\times$ the SM rate.

- **Point 3** has $m_{h_1^0} = 99.7$ GeV and $m_{a_1} = 20.4$ GeV.

  The dominant final state is $h_1 \to a_1 a_1 \to b\overline{b}b\overline{b}$.

  From the table, we extract $C^2(b\overline{b}b\overline{b}) = [g^2_{Zh_1}/g^2_{Zh_{\rm SM}}] \times BR(h_1 \to a_1 a_1) \times [BR(a_1 \to b\overline{b}]^2 \sim 0.8$.

  This barely sneaks below the relevant contour of Fig. 3.

  This is a canonical example of a point for which one could look for the above final state in gg or WW fusion, or Wh associated production, using b tagging.

- The $m_{h_1^0}$ values for $\boxed{\text{points 4 and 5}}$ are somewhat higher (and certainly beyond all LEP limits) and production rates for the h_1 (even though essentially of SM strength) would be somewhat lower.

  Still, these kinds of points with dominant $a_1 a_1 \to b\bar{b}b\bar{b}$ final state might be interesting because of the possibility of using b-tagging.

- Moving on, the next really interesting point in the tables is $\boxed{\text{point 7}}$.

  Here we have a rather low $m_{h_1^0} \sim 69.5~\mathrm{GeV}$ matched with a fairly high $m_{a_1} \sim 32.9~\mathrm{GeV}$.

  The dominant decay mode is $h_1 \to a_1 a_1 \to b\bar{b}b\bar{b}$ with $C^2(b\bar{b}b\bar{b}) \sim 0.22$.

  This again falls slightly below the relevant contour of Fig. 3 and well below the limit of Fig. 4.

  Despite the 0.32 and 0.38 suppression factors for WW and gg fusion respectively (relative to the SM rates), the low mass implies substantial SM rates to begin with and b tagging could yield a signal.

- Now let us examine $\boxed{\textbf{point 9}}$ with $m_{h_1^0} \sim 39.8~\mathrm{GeV}$ and $m_{a_1} \gg m_{h_1^0}$.

  This h_1 is mainly singlet and has very tiny ZZ coupling. However, its $b\bar{b}$ coupling is 0.352 of SM strength and so production and detection in the $gg \to b\bar{b}h_1 \to b\bar{b}b\bar{b}$ mode might be worth examining.

  The h_2 is the (very) SM-like guy in this case, and decays primarily via $h_2 \to h_1 h_1 \to b\bar{b}b\bar{b}$.

  Since $m_{h_2} \sim 125~\mathrm{GeV}$, there is no problem with LEP limits, but the Tevatron cross sections would not be large.

Point Number	10	11	12	13	14
Bare Parameters					
λ	0.390	0.500	0.270	0.373	0.411
κ	0.183	$-.152$	0.147	0.243	$-.184$
$\tan\beta$	3.50	3.50	2.86	3.36	2.42
$\mu_{\rm eff}$	-245.0	200.0	-753.0	-315.0	184.0
A_λ	-230.0	780.0	312.0	171.0	626.0
A_κ	-5.0	230.0	8.4	52.1	32.8
CP-even Higgs Boson Masses and Couplings					
m_{h_1} (GeV)	94.1	57.3	95.4	88.0	113.8
R_1	0.945	-0.278	0.997	0.980	-0.992
t_1	0.949	-0.301	0.991	0.966	-0.989
b_1	0.890	0.015	1.047	1.135	-1.011
g_1	0.952	0.326	0.988	0.957	0.988
$B(h_1 \to b\overline{b})$	0.047	0.055	0.003	0.001	0.007
$B(h_1 \to \tau^+\tau^-)$	0.004	0.003	0.000	0.000	0.001
$B(h_1 \to c\overline{c} + s\overline{s} + gg)$	0.005	0.933	0.000	0.000	0.001
$B(h_1 \to a_1 a_1)$	0.943	0.000	0.996	0.999	0.991
m_{h_2} (GeV)	239.5	124.7	483.1	198.5	168.9
R_2	-0.327	-0.961	-0.014	-0.026	-0.122
t_2	-0.299	-0.952	-0.364	-0.321	-0.085
b_2	-0.669	-1.066	2.843	3.314	-0.339
g_2	0.295	0.948	0.366	0.384	0.080
$B(h_2 \to b\overline{b})$	0.002	0.048	0.020	0.060	0.004
$B(h_2 \to \tau^+\tau^-)$	0.000	0.004	0.002	0.007	0.000
$B(h_2 \to W^+W^- + ZZ)$	0.437	0.012	0.003	0.001	0.050
$B(h_2 \to a_1 a_1)$	0.246	0.000	0.002	0.079	0.944
$B(h_2 \to h_1 h_1)$	0.314	0.930	0.010	0.007	0.000
$B(h_2 \to a_1 Z)$	0.000	0.000	0.485	0.845	0.002

Table 6: Properties of points for which the $WW \to h_H \to h_L h_L \to jj\tau^+\tau^-$ modes don't work.

Point Number	10	11	12	13	14
CP-odd Higgs Boson Masses and Couplings					
m_{a_1} (GeV)	40.0	188.2	1.3	3.4	1.9
t_1'	0.000	0.044	0.076	0.204	0.081
b_1'	0.000	0.534	0.624	2.303	0.473
g_1'	0.000	0.038	0.363	1.003	0.197
$B(a_1 \to b\bar{b})$	0.015	0.007	0.000	0.000	0.000
$B(a_1 \to \tau^+\tau^-)$	0.001	0.001	0.000	0.000	0.000
$B(a_1 \to c\bar{c} + s\bar{s} + gg)$	0.000	0.000	0.948	0.938	0.936
$B(a_1 \to \gamma\gamma)$	0.983	0.000	0.000	0.000	0.000
$B(a_1 \to \widetilde{\chi}_1^0\widetilde{\chi}_1^0)$	0.000	0.992	0.000	0.000	0.000

Table 7: Properties (continued) of selected scenarios for which LHC Higgs detection would not even be possible in the $WW \to h_H \to h_L h_L \to jj\tau^+\tau^-$ modes.

Discussion of points 10 to 14: no $a_1 \to b\bar{b}$ decays

- **Point 10** provides something quite unique.

  The h_1 with $m_{h_1^0} \sim 94.1~\mathrm{GeV}$ is quite SM-like, but it decays via $h_1 \to a_1 a_1 \to \gamma\gamma\gamma\gamma$ as the dominant final state, with an effective $C^2 \sim 0.82$.

  The possibility of reconstructing each a_1 in the $\gamma\gamma$ channel at $m_{a_1} \sim 40~\mathrm{GeV}$ should give a really clean signature.

  Searches for this kind of unusual signal should not be ignored!

- The next point that presents something quite new and might be accessible at the Tevatron is $\boxed{\text{point 11}}$, with $m_{h_1^0} = 57.3$ GeV and $m_{h_2} = 124.7$ GeV.

  Because of an accidental suppression of the $h_1 b\overline{b}$ coupling, the dominant h_1 decay is to $c\overline{c} + s\overline{s} + gg$ (mainly $c\overline{c}$).

  This escapes LEP limits in the Zjj final state because the effective $C^2(jj) = [g^2_{Zh_1}/g^2_{Zh_{\rm SM}}] \times BR(h_1 \to jj) \sim 0.07$ falls below (but, as usual, not by much) the 95% CL limit for this quantity at $m_{h_1^0} \sim 57.3$ GeV from the $Zh \to Zjj$ LEP searches, as plotted in Fig. 11.

  (This dedicated search provides the strongest limits for this kind of case.)

  This same suppression factor would apply to $WW \to h_1 \to jj$ searches and triggering on the c's in the final state would be inefficient.

  Thus, to us, it looks hard.

  Meanwhile, there is also the $h_2 \to h_1 h_1 \to jjjj$ possibility, but the high $m_{h_2} \sim 124.7$ GeV coupled with no b's probably makes this one hard too.

- $\boxed{\text{Points 12, 13 and 14}}$ are all characterized by a SM-like h_1 with masses of $m_{h_1^0} \sim \mathbf{95.4}$ GeV, $\mathbf{88}$ GeV and $\mathbf{113.8}$ GeV, respectively, decaying via $h_1 \to a_1 a_1$ with each a_1 decaying to $c\overline{c} + s\overline{s} + gg$.

Because the $m_{h_1^0}$ values are beyond the specialized LEP limits, these are all allowed scenarios. One would need to look for WW or gg fusion to h_1 followed by h_1 decays as specified above.

Again, this is likely to be difficult because of the lack of b or τ tagging.

Conclusions

We believe that these scenarios represent test cases of real importance at the Tevatron.

- The NMSSM is an attractive model, and the $h \to aa$ decay modes have significantly nice features with regard to finetuning and electroweak baryogenesis.

- The sometimes modest Higgs masses involved and the typically fairly SM-like couplings of the primary Higgs mean that the Tevatron production rates are significant. Further, the smaller backgrounds at the Tevatron might make it possible to see these Higgs-to-Higgs pair signals before the LHC turns on if efficient background reduction techniques can be found.

- There are lots of NMSSM Higgs scenarios, and it will probably take years to place limits or detect a weak signal, but hopefully not more years than we have left before LHC turn-on.